

Supplementary Materials

Vince Buffalo and Andrew Kern

June 27, 2023

Contents

1	Quantitative Genetic Linked Selection Model Theory	2
1.1	Sources of Neutral Allele Frequency Change	2
1.2	The Variance in Neutral Allele Frequency Change	3
1.3	Heritable Fitness and the Accumulation of Autocovariance	4
1.4	The Draft-Effective Population Size	8
1.5	The Draft-Effective Population Size Under Polygenic Selection	8
1.6	Continuous Approximation to the Segment Under Selection	9
1.7	The Variance Dynamics	11
1.8	The Draft-Effective Population Size Under Strong Background Selection	11
1.9	Draft-Effective Population Size Under Weak and Strong BGS	12
2	Statistical Methods	14
2.1	Parametric Forms of Negative Linked Selection Models	14
2.1.1	Reductions Under the Classic BGS Model	15
2.1.2	Reduction Under the Modified Santiago and Caballero Model	16
2.2	Discretization of Parameters and Annotation Feature Classes	16
2.3	Data Summary Matrices	17
2.4	Pairwise Diversity Estimates	18
2.5	Window-based Summaries and filtering	19
2.6	Annotation Models	19
2.7	Ratchet Rate Prediction	19
2.8	Numeric Optimization	20
2.9	Numeric methods for calculating B	20
2.10	Optimization	20
3	Human Genomic Data	20
3.1	20
3.2	Filtering gVCFs	20
3.3	Non-accessible and Masked Regions	21
3.4	Putatively Neutral Tracks	21
3.5	Model Comparisons	22
3.6	Table of R^2 Values	22
3.7	Derivation of Approximate Drift R^2	22

3.8	Predicted Rate of Fitness Change	26
3.9	Likelihood	27
3.10	The scale of processes	28
4	Simulations	29
4.1	Segment Simulations	29
5	Additional Results and Figures	29
5.1	Chromosome Fit Figures	29

1 Quantitative Genetic Linked Selection Model Theory

1.1 Sources of Neutral Allele Frequency Change

Here, we step through a quick derivation of Santiago and Caballero (1995). Throughout, we assume random mating, hermaphroditic individuals, and a constant population size. The change in a neutral allele's frequency in one generation can be partitioned into the three sources of stochasticity: the random associations with fitness backgrounds (i.e. *draft*), the non-heritable randomness in family size, and the Mendelian noise from heterozygotes segregating. If we let $x_{0,i} \in \{0, 1/2, 1\}$ be the frequency of neutral alleles individual i in generation 0 carries, we can partition the random neutral allele frequency of the population (x_t without the individual index) into the underlying stochastic causes,

$$x_1 = \frac{1}{2N} \sum_{i=1}^N \left(x_{0,i} k_{0,i} + \sum_{j=1}^{k_{0,i}} \delta_{0,i,j} \right) \quad (1)$$

where $k_{0,i}$ is the number of surviving gametes parent i passes on, and $\delta_{0,i,j}$ is a random term that encapsulates the noise due to Mendelian segregation of heterozygotes. If parent i is a homozygote ($x_{0,i} \in \{0, 1\}$), then $\delta_{0,i,j} = 0$, whereas if $x_{0,i} = 1/2$ then $\delta_{0,i,j} = \pm 1/2$ with equal probability. This is because a heterozygous parent will transmit half a neutral allele in expectation, but each round of Mendelian segregation must pass on either 0 or 1 alleles, which the random $\pm 1/2$ term imposes. The factor of $1/2$ is due to the fact that we're summing over N diploids, but considering the number of gametes they transmit. Since each diploid parent must have two offspring to maintain a constant population size, $1/N \sum_i k_{0,i} = 2$.

The frequency in the initial generation is $x_0 = 1/N \sum_{i=1}^N x_{0,i}$, though to indicate that we treat this as fixed rather than random, we use $p_0 := x_0$. Then, the allele frequency change is,

$$\begin{aligned} \Delta x_1 = x_1 - p_0 &= \frac{1}{2N} \sum_{i=1}^N x_{0,i} (k_{0,i} - 1) + \frac{1}{2N} \sum_{i=1}^N \sum_{j=1}^{k_{0,i}} \delta_{0,i,j} \\ \Delta x_1 &= K_1 + H_1 \end{aligned} \quad (2)$$

where K_1 and H_1 are the random change in neutral allele frequency change due to offspring number (including heritable and non-heritable components), and Mendelian segregation in generation 1.

1.2 The Variance in Neutral Allele Frequency Change

Now, let us look the variance of $V(\Delta x_1)$ over evolutionary replicates. Since the Mendelian segregation and the offspring random process are independent,

$$V(\Delta x_1) = V(K_1) + V(H_1). \quad (3)$$

Looking at each term,

$$V(K_1) \approx \frac{1}{4N^2} \sum_{i=1}^N V(x_{0,i}(k_{0,i} - 1)) \quad (4)$$

where we ignore the covariance terms due to the sum, since these are on order $1/N^3$. In the first generation from an arbitrary starting point, the neutral alleles assort independently into diploids with respect to their fitness, so we can simplify the variance as

$$\begin{aligned} V(K_1) &\approx \frac{1}{4N^2} \sum_{i=1}^N V(x_{0,i})V(k_{0,i} - 1) \\ &\approx \frac{1}{4N} V(x_{0,i})V(k_{0,i}). \end{aligned} \quad (5)$$

Assuming no correlation between parental gametes (e.g. no inbreeding), $V(x_{0,i})$ is the binomial variance in individual allele frequency, or $p_0(1 - p_0)/2$, and $V(k) := V(k_{0,i})$ is the offspring variance of an individual given by the reproduction process. For example, if the reproduction process is a neutral multinomial Wright–Fisher, $V(k) \approx 2$. Then, the variance in allele frequency change due to non-heritable offspring number variation is,

$$V(K_1) \approx \frac{p_0(1 - p_0)}{2N} \frac{V(k)}{4}. \quad (6)$$

The Mendelian noise variance term can be derived similarly. First, the sum over each parent's transmitted gametes can be simplified by noting that parents are exchangeable over evolutionary replicates with respect to their contribution to this term. In a constant population size, the double summation over parents and their offspring can be replaced by a summation over offspring, since both sum N exchangeable terms. Then, note that $V(\delta_{i,j}) = 1/4 p_0(1 - p_0)$, so

$$V(H_1) = \frac{p_0(1 - p_0)}{2N} \frac{1}{2}. \quad (7)$$

Finally, we have

$$V(\Delta x_1) = V(K_1) + V(H_1) \quad (8)$$

$$\begin{aligned} &\approx \frac{p_0(1 - p_0)}{2N} \frac{V(k)}{4} + \frac{p_0(1 - p_0)}{2N} \frac{1}{2} \\ &\approx \frac{p_0(1 - p_0)}{2N} \left(\frac{V(k)}{4} + \frac{1}{2} \right) \end{aligned} \quad (9)$$

(c.f. Santiago and Caballero 1995 equation 2 and Buffalo and Coop 2019 equation 30). Note that if the reproduction process is a neutral multinomial Wright–Fisher, $V(k) \approx 2$, and this simplifies to the expected Wright–Fisher variance. If we were to define a variance *drift-effective* population size N_e by setting this variance in neutral allele frequency change to the expected variance under a Wright–Fisher model (V_{WF}), we’d have

$$\begin{aligned} V_{WF} &:= \frac{p_0(1-p_0)}{2N_e} \\ V_{WF} &= V(\Delta p_1) \\ N_e &= \frac{4N}{V(k) + 2} \end{aligned} \tag{10}$$

(c.f. Wright 1938).

Now, we look at the variance in allele frequency change across two generations for a neutral allele. The change in neutral allele frequency, regardless of the selective system, is directionless in expectation. This is because whichever allele we track is arbitrary by the definition of neutrality, which imposes a symmetry, $\mathbb{E}(\Delta x) = 0$. Then, the variance of change in the first generation is,

$$V(\Delta x_1) = \mathbb{E}_1 [(x_1 - x_0)^2] = \frac{x_0(1-x_0)}{2N}, \tag{11}$$

and across two generations,

$$\begin{aligned} V(x_2 - x_0) &= \mathbb{E} [(x_2 - x_0)^2] \\ &= \mathbb{E}_1 [\mathbb{E}_2 [((x_2 - x_1) + (x_1 - x_0))^2 | x_1]] \\ &= \mathbb{E}_1 [\mathbb{E}_2 [(\Delta x_2 + \Delta x_1)^2 | x_1]] \\ &= \mathbb{E}_1 [\mathbb{E}_2 [\Delta x_2^2 | x_1]] + \mathbb{E}_1 [\Delta x_1^2] + 2\mathbb{E}_1 [\mathbb{E}_2 [\Delta x_2 \Delta x_1 | x_1]] \\ &= \mathbb{E}_1 [\mathbb{E}_2 [\Delta x_2^2 | x_1]] + \mathbb{E}_1 [\Delta x_1^2] + 2\mathcal{C}_{1,2} \\ &= \frac{p_0(1-p_0)}{2N} \left(1 - \frac{1}{2N}\right) + \frac{p_0(1-p_0)}{2N} + 2\mathcal{C}_{1,2} \end{aligned} \tag{12}$$

Consequently, the variance of the neutral allele frequency changes each generation according to the probability of failing to coalesce each generation and the pairwise covariance terms $\mathcal{C}_{i,j}$ that build up due to associations with heritable fitness backgrounds. Note that the covariance term $\mathcal{C}_{1,2} = \mathbb{E}_1 [\mathbb{E}_2 [\Delta x_2 \Delta x_1 | x_1]] = 0$ when there is no heritable fitness variation, and this simplifies to the well-known equation for variance in a Wright–Fisher population.

1.3 Heritable Fitness and the Accumulation of Autocovariance

Next, we turn our attention to the case where there is heritable fitness variation, which leads to non-zero covariance terms $\mathcal{C}_{i,j}$. These terms emerge when $V(k)$ has a heritable component of fitness that can be transmitted along with the neutral allele, thereby affecting the neutral allele’s trajectory in later generations. If we partition the offspring number into heritable and non-heritable

components, $k_i = 2f_i + \varepsilon_i$, then $V(k_i) = 4V_A + V_n$. When there is heritable fitness variation across individuals, $V_A > 0$. Because the population size is assumed to be constant, the mean heritable fitness across individuals is constrained to be $\mathbb{E}_i(f_i) = 1$; this implies that the individual fitness values f_i are relative fitnesses as is standard in population genetics, in this case to the population mean. Thus V_A is the squared coefficient of heritable fitness variation (this is often denoted as $C^2 = V_A/\bar{w}^2$, see Charlesworth 1987; Crow 1958; Houle 1992).

We can further decompose the K_1 term into $K_1 = S_1 + D_1$,

$$\begin{aligned} V(\Delta x_1) &= V(S_1) + V(D_1) + V(H_1) \\ &\approx \frac{p_0(1-p_0)}{2N} V_A + \frac{p_0(1-p_0)}{2N} \frac{V_n}{4} + \frac{p_0(1-p_0)}{2N} \frac{1}{2} \end{aligned} \quad (13)$$

(c.f. Santiago and Caballero 1995 equation 11).

To see how the covariance terms accumulate, consider $V(x_3 - p_0)$. Note that $\mathbb{E}(S_t) = \mathbb{E}(D_t) = \mathbb{E}(H_3) = 0$, since which neutral allele we track is arbitrary, so by symmetry the expected change is zero. Then,

$$\begin{aligned} V(x_3 - p_0) &= \mathbb{E} \left[(S_1 + D_1 + H_1 + S_2 + D_2 + H_2 + S_3 + D_3 + H_3)^2 \right] \\ &= \mathbb{E}(S_1^2) + \mathbb{E}(S_2^2) + \mathbb{E}(S_3^2) \\ &\quad + \mathbb{E}(S_1 S_2) + \mathbb{E}(S_1 S_3) + \mathbb{E}(S_2 S_3) \\ &\quad + \mathbb{E}(D_1^2) + \mathbb{E}(H_1^2) + \mathbb{E}(D_2^2) + \mathbb{E}(H_2^2) + \mathbb{E}(D_3^2) + \mathbb{E}(H_3^2). \end{aligned} \quad (14)$$

The covariance terms $\mathbb{E}(S_i S_j)$ for $j > i$ represent the expected neutral allele frequency change from a neutral allele becoming associated with a fitness background in generation i and that fitness association persisting until generation j . However, the covariances terms $\mathbb{E}(S_j S_i)$ for $j > i$ are zero since associations in the future cannot affect the past (see p. 1041 of Buffalo and Coop 2019). Let us consider S_1 and S_2 . We have,

$$\begin{aligned} S_1 &= \frac{1}{2N} \sum_{i=1}^N x_{0,i} (f_{0,i} - 1) = \text{cov}(x_{0,i}, f_{0,i}) \\ S_2 &= \frac{1}{2N} \sum_{i=1}^N x_{1,i} (f_{1,i} - 1) = \text{cov}(x_{1,i}, f_{0,i}) \end{aligned} \quad (15)$$

which are chance covariances (across the population, *not* evolutionary replicates) created by the random sorting of neutral alleles and fitness into individuals, *each generation*. These covariances are equivalent to the Robertson-Price equation (Price 1970; Robertson 1966), which predict the change in neutral frequency due to heritable fitness (and likewise with the change due to non-heritable factors).

Considering the underlying haplotypes that lead to $x_{0,i}$ and $f_{0,i}$ can give us an equation for the dynamics of the $\mathbb{E}(S_i S_j)$ (for $j > i$) terms over evolutionary replicates. Let us partition the allele frequency and fitness by into the average of the paternal contributions. The neutral allele frequency per gamete is either 0 or 1, and we assume the fitnesses across gametes are additive.

Then, as long as there is random mating, we can simplify the associations in a diploid by looking at a single gamete,

$$\begin{aligned}
S_1 &= \text{cov}(x_{0,i}, f_{0,i}) = \text{cov}\left(\frac{x'_{0,i} + x''_{0,i}}{2}, f'_{0,i} + f''_{0,i}\right) \\
&= \frac{1}{2} (\text{cov}(x'_{0,i}, f'_{0,i} + f''_{0,i}) + \text{cov}(x''_{0,i}, f'_{0,i} + f''_{0,i})) \\
&= \text{cov}(x'_{0,i}, f'_{0,i} + f''_{0,i}) \\
&= \text{cov}(x'_{0,i}, f'_{0,i}) + \text{cov}(x'_{0,i}, f''_{0,i}) \\
&= S'_1 + S''_1
\end{aligned} \tag{16}$$

which follows from symmetry again, since it does not matter which gamete carrying the neutral allele we track (c.f. Santiago and Caballero 1998 p. 2107). The primes now indicate whether the selected locus is on the same gamete as the neutral allele (single prime), or the homologous gamete (double prime).

After meiosis, a fraction $1 - r$ of these associations between the tracked neutral allele $x'_{0,1}$ and fitness background $f'_{0,i}$ persist, and a fraction r disassociate its currently coupled background and create an association with the homologous fitness background, $f''_{0,i}$. When linkage is tight, this latter term can be ignored as we will do here, though it does impact background levels of neutral diversity (Santiago and Caballero 1995). Additionally, the fitness effects of the selected background may change in later generations, in complex ways (Barton 1986; Turelli and Barton 1990). Santiago and Caballero (1995) assume an equilibrium level of fitness variation V_A , with the fitness variance associated with a particular background decaying at a simple geometric decay at rate $1 - \kappa$ each generation, which is sufficient for background selection. An approximate rate of the decay can be worked out for the particular selective system. In general, this can be a much more complicated function; Buffalo and Coop (2019) show that even fluctuating selection can be accommodated.

Now, the associations created in generation 1 and that persist in future generations as (ignoring S''_i terms) follow the pattern

$$\begin{aligned}
S'_2 &= S_1(1 - \kappa)(1 - r) \\
S'_3 &= S_1(1 - \kappa)^2(1 - r)^2 \\
S'_4 &= S_1(1 - \kappa)^3(1 - r)^3.
\end{aligned} \tag{17}$$

Then, the cumulative effect of the fitness associations created in generation 1 can be written as,

$$\begin{aligned}
S_1 Q_t &= S_1 + S'_2 + S'_3 + \dots + S'_t \\
Q_t &= 1 + \sum_{i=1}^t (1 - r)^i (1 - \kappa)^i
\end{aligned} \tag{18}$$

or for continuous t ,

$$Q_t = 1 + \frac{(1 - \kappa)(1 - r) (1 - (1 - \kappa)^t (1 - r)^t)}{\kappa + (1 - \kappa)r} \tag{19}$$

which as $t \rightarrow \infty$, converges to,

$$Q_\infty = \frac{1}{\kappa + r(1 - \kappa)}. \quad (20)$$

This shows the long reach of heritable fitness factors in altering allele frequency through the generations. In terms like $\mathbb{E}(S_1 S_2)$, a fraction S'_1 of the heritable allele frequency change S_2 were *previously* built associations between the neutral allele and a fitness background from S_1 . As long as the direction of selection is the same, the expected change of this fraction of associations formed in the first generation to later generations 2 and 3 would be,

$$\begin{aligned} \mathbb{E}(S_1 S_2) &= \mathbb{E}(S_1^2)(1 - \kappa)(1 - r) = \mathbb{E}(S_1^2)Q_2^2 \\ \mathbb{E}(S_1 S_3) &= \mathbb{E}(S_1^2)(1 - \kappa)^2(1 - r)^2 = \mathbb{E}(S_1^2)Q_3^2. \end{aligned} \quad (21)$$

The Q_t^2 terms represent the inflation of variance due to autocovariance in frequency change across generations due to weak draft.

With these covariance terms, we now have a full model for $V(p_t - p_0)$. We will look at the case for $t = 2$. As shown in Supplementary Equation (13), the second moment of every term is a function of the variance in neutral allele frequency in that generation, $x_t(1 - x_t)$. This variance does not stay its initial value of $x_0(1 - x_0)$; it decays each generation due to coalescence from the drift and selection processes modeled by this approach. The rate at which this decay happens is the effective population size each generation implied by this model. We can write,

$$\begin{aligned} V(x_2 - p_0) &= \mathbb{E}(S_1^2) + \mathbb{E}(S_1 S_2) + \mathbb{E}(S_2^2) \\ &\quad + \mathbb{E}(D_1^2) + \mathbb{E}(H_1^2) + \mathbb{E}(D_2^2) + \mathbb{E}(H_2^2) \\ \frac{V(x_2 - p_0)}{p_0(1 - p_0)} &= \frac{V_A}{2N} + \frac{V_A Q_2^2}{2N} \left(1 - \frac{1}{2N}\right) + \frac{V_A}{2N \left(1 - \frac{1}{2N}\right)} \\ &\quad + \frac{V_n}{8N} + \frac{1}{4N} + \frac{V_n}{8N} \left(1 - \frac{1}{2N}\right) + \frac{1}{4N} \left(1 - \frac{1}{2N}\right). \end{aligned} \quad (22)$$

In general, the variance in allele frequency change after t generations in a system with heritable fitness due to a single locus r recombination fraction away from the neutral site is given by,

$$\frac{V(x_t - p_0)}{p_0(1 - p_0)} = \sum_{i=1}^t \frac{1}{2N} \left(V_A Q_i^2 + \frac{V_n}{4} + \frac{1}{2} \right) \left(1 - \frac{1}{2N} \right)^{i-1}. \quad (23)$$

We will see later that with the appropriate form for Q_t^2 , this equation holds for polygenic selection (see Supplementary Section 1.5). Additionally, we note that since the probability of coalescence (or, equivalently, identity by descent) is proportional to the variance in allele frequency change (Barton 2000), this equation for the variance encodes the pairwise coalescent rate of the population through time under weak draft. Others have found that the genealogies under purifying selection can be characterized by such a time-dependent effective population size (Nicolaisen and Desai 2013).

1.4 The Draft-Effective Population Size

Now, we consider how to turn this expression for the variance in neutral allele frequency at time t under weak draft into an expression for the *draft-effective* population size analogous to Supplementary Equation (10). In an ideal Wright–Fisher population, the instantaneous variance is $V(\Delta x_t) = p_{t-1}(1-p_{t-1})/2N_{d,t-1}$. Santiago and Caballero consider the allele frequency change at some t to define their effective population size at time t (which we here are calling draft-effective population size, $N_{d,t}$),

$$N_{d,t} := \frac{p_{t-1}(1-p_{t-1})}{2V(x_t) - V(x_{t-1})}. \quad (24)$$

The time-dependency is due to Q_t^2 , which reflects the fact that autocovariances build up, but at a decreasing rate. Note that levels of pairwise diversity depend on the full distribution of pairwise coalescence times, or the $N_{d,t}$ (e.g. see equation 4 of Santiago and Caballero 2016 and equation 16 of Santiago and Caballero 1998).

Using Supplementary Equation (23) we have,

$$N_{d,t} \approx \frac{4N}{4V_A Q_t^2 + V_n + 2} \quad (25)$$

(cf. equation 18, Santiago and Caballero 1995). Note if $V_A = 0$, this equation reduces to Wright’s (1938) equation.

In many cases, we care about the asymptotic N_d ,

$$N_d := \lim_{t \rightarrow \infty} N_{d,t} \approx \frac{4N}{4V_A Q_\infty^2 + V_n + 2}. \quad (26)$$

We now turn to different expressions for Q_t^2 and V_A .

1.5 The Draft-Effective Population Size Under Polygenic Selection

The results of the previous section assume only a single locus a recombination fraction r apart from the neutral locus is determining the coalescence rate. The model of Santiago and Caballero (1998) extends this to the case where fitness is polygenic. As they show in their original paper, this system can accommodate a variety of different equilibrium selection systems as long as expressions for V_A and $1 - \kappa$ can be worked out. Other authors have extended similar models to more elaborate breeding structures (Woolliams et al. 1993; Wray and Thompson 1990).

First, we extend Supplementary Equation (25) to a polygenic system. Throughout, we assume a multiplicative fitness model (i.e. independent effects, no epistasis), where the fitness of individual i is the product of their fitness contributions from each locus l , $w_{i,l}$, giving $w_i = \prod_{l=1}^n w_{i,l}$. Then, assuming mean fitness is one and independence between sites, the total fitness variation is multiplicative across the locus-level fitnesses,

$$V_A = \prod_{l=1}^n (1 + V_{h,l}) - 1 \quad (27)$$

Similarly, the $Q_t^2 V_A$ term in the single-locus model is multiplicative under the polygenic model, as the change in site-specific fitness variances are assumed independent,

$$Q_t^2 V_A = \prod_{l=1}^n \left(1 + \frac{V_{h,l} Q_{t,l}^2}{2} \right) - 1 \quad (28)$$

where $Q_{t,l}$ is the cumulative impact of selection due to the selected site l (c.f. equation 4 Santiago and Caballero 1998). The factor of $1/2$ is due to the fact that we are ignoring the chance that the fitness background on the homologous chromosome recombines onto the haplotype with the tracked neutral allele (i.e. due to the Q_t'' associations). In other words, only half the fitness variation in a diploid can stay associated with the neutral allele through the generations.

To simplify the derivation, assume $V_n = 2$ as under a Wright–Fisher model. Then, the effective population size is,

$$\begin{aligned} N_{d,t} &\approx \frac{N}{V_A Q_t^2 + 1} \\ &\approx \frac{N}{\prod_{l=1}^n \left(1 + \frac{V_{h,l} Q_{t,l}^2}{2} \right)} \\ &\approx N \exp \left(- \sum_{l=1}^n \frac{V_{h,l} Q_{t,l}^2}{2} \right) \end{aligned} \quad (29)$$

(c.f. Santiago and Caballero 1998 equation 4b). If we write each site l 's contribution to the variance as a deviation from the average contribution, $V_{h,l}^2 = 1/n V_A + \epsilon_l$, then

$$\begin{aligned} N_{d,t} &\approx N \exp \left(- \frac{1}{2} \sum_{l=1}^n \left(\frac{1}{n} V_h + \epsilon_l \right) Q_{t,l}^2 \right) \\ &\approx N \exp \left(- \frac{V_h}{2n} \sum_{l=1}^n Q_{t,l}^2 + \sum_{l=1}^n \epsilon_l Q_{t,l}^2 \right) \end{aligned} \quad (30)$$

Santiago and Caballero assume that over evolutionary replicates, as selected sites are randomly distributed, there is not systematic covariance between the fitness variation at a site and the decay of its association with the neutral site, e.g. $\mathbb{E}(\epsilon_l Q_{t,l}^2) = 0$, and thus ignore the second sum term, leading to

$$N_{d,t} \approx N \exp \left(- \frac{V_h}{2n} \sum_{l=1}^n Q_{t,l}^2 \right). \quad (31)$$

1.6 Continuous Approximation to the Segment Under Selection

Our model differs from that of Santiago and Caballero (1998) in that we do not integrate over the entire genome. In their 1998 model, Santiago and Caballero consider the impact of both sites

under selection on the same chromosome, as well as sites on independently assorting chromosomes. We only consider the contribution of a single segment under purifying selection, and the reduction from additional segments accumulate multiplicatively. Like their model, we imagine the reduction experienced by a focal neutral site in the middle of the segment. The implementation of our method differs slightly on though, see XXX.

The $Q_{t,l}$ terms depend on l only through the recombination fraction $r(l)$ between the neutral allele and the selected site. Assuming a constant per-basepair recombination rate of r_{BP} , $r(l) = r_{BP}l$ we can approximate the sum with an integral for the asymptotic Q_∞ . The reduction experienced in the middle of a chromosome is twice the reduction experienced from each half,

$$\begin{aligned} N_{d,\infty} &\approx N \exp \left(-\frac{V_h}{2L} \sum_{l=1}^L Q_{\infty,l}^2 \right) \\ &\approx N \exp \left(-\frac{V_h}{M} \int_0^{M/2} Q_\infty(r)^2 dr \right) \end{aligned} \quad (32)$$

where $M = nr_{BP}$ is the total segment length in Morgans. Then, the total asymptotic effect of associations from all sites as Q_∞^2 . Then,

$$\begin{aligned} Q_\infty^2 &= \frac{2}{M} \int_0^{M/2} Q_\infty(r)^2 dr \\ &= \frac{2}{M} \int_0^{M/2} \left(\frac{1}{1 - (1-r)Z} \right)^2 dr. \\ &= \frac{2}{(1-Z)(2 - (2-M)Z)} \end{aligned} \quad (33)$$

Santiago and Caballero further approximate this; we can derive their approximation by setting $Z = 1 - \kappa$ and doing a first-order Taylor series expansion around κ (since the loss in variance is presumed to be small). Then,

$$Q_\infty^2 = \frac{2}{M(1-Z)} + \frac{2(M-2)}{M^2} + \frac{2(M^2 - 4M + 4)(1-Z)}{M^3} + \mathcal{O}(\kappa^2) \quad (34)$$

Santiago and Caballero's approximation only keeps this first term, e.g. their $Q_\infty^2 \approx 2/(M(1-Z))$, which is only accurate in the domain $M > 0.2$.

$$N_{d,\infty}^{(SC98)} \approx N \exp \left(-\frac{V_A}{(1-Z)M} \right) \quad (35)$$

(c.f. Santiago and Caballero 1998 equation 8). For small M , the small κ approximation strongly deviates from the full equation; thus, throughout, we use the unapproximated version,

$$N_{d,\infty} \approx N \exp \left(-\frac{V_A}{(1-Z)(2 - (2-M)Z)} \right). \quad (36)$$

For the reasons described earlier, a single asymptotic $N_{d,\infty}$ cannot fully characterize pairwise coalescent rates in all cases, and thus neutral diversity levels depend on the full $N_{d,t}$, for which we integrate equation (19) to get,

$$N_{d,t} \approx N \exp \left(-\frac{V_A}{M} \int_0^{M/2} \left(1 + \frac{(1-k)(1-r)(1-(1-k)^t(1-r)^t)}{k+(1-k)r} \right) dr \right). \quad (37)$$

1.7 The Variance Dynamics

The heritable variance in fitness V_A associated with the tracked neutral allele does not remain constant through the generations, but decays due to selection and drift, and is maintained by the input of new mutations. For an arbitrary polygenic selective system, the dynamics are extraordinarily complicated due to the complexity of multilocus selection, and the dynamics of the trait response to selection depend on the variance, which in turn depends on higher moments of the fitness distribution (the “moment-closure problem”). We discuss the simplification of Santiago and Caballero’s model here.

Each generation, the genetic variance changes due to changes in the allele frequencies at selected sites and linkage disequilibria between these sites. These are typically expressed as recursions, but certain models permit these changes to be expressed as a proportional reduction (e.g. truncation selection and stabilizing selection models; Keightley and Hill 1988 p. 36, and Walsh and Lynch 2018 p. 557). Santiago and Caballero’s model follows this approach, assuming the variance decays due to selection and drift at a constant rate $Z := 1 - \kappa$ through the generations, such that the variance in the next generation excluding mutation is $V'_A = (1 - \kappa)V_A$ and $\Delta V_A = -\kappa V_A$.

With mutation, $\Delta V_A = V_m - \kappa V_A$. The model of Santiago and Caballero assumes that under the long-run equilibrium, $\Delta V_A = 0$, such that $\kappa V_A = V_m$, and thus the rate of loss is $\kappa = V_m/V_A$. Then the variance for the dynamics simplify to,

$$\begin{aligned} V'_A &= \left(1 - \frac{V_m}{V_A} \right) V_A \\ Z &:= \frac{V'_A}{V_A} = 1 - \kappa = 1 - \frac{V_m}{V_A} \end{aligned} \quad (38)$$

(c.f. Santiago and Caballero 1998 equation 9).

1.8 The Draft-Effective Population Size Under Strong Background Selection

Under strong background selection, multiple segregating deleterious sites contribute to fitness variation. BGS models assume a multiplicative fitness model, such that the fitness of an individual is

$$w = (1 - s)^n \quad (39)$$

where n is the number of deleterious mutations this individual carries.

Classic background selection theory assumes an infinite population size, such that mutation frequencies are at their mutation-selection equilibrium and the expected number of mutations across

individuals is $\mathbb{E}(n) = \mu/sL$ where L is the total number of basepairs that can be mutated (the mutational target size). Under a multiplicative fitness function in an infinite population, selection cannot generate linkage disequilibria (Turelli and Barton 1990). Thus the classic strong background selection model assumes additive genetic fitness is equal to the additive genic fitness (which excludes the contribution of covariance between selected sites),

$$\begin{aligned} V_{\text{BGS}} &:= V(w) = 2s^2 \sum_{l=1}^L p_l(1 - p_l) \\ &= 2Ls^2 \frac{\mu}{s} \left(1 - \frac{\mu}{s}\right) = Us + \mathcal{O}(\mu^2) \approx Us. \end{aligned} \quad (40)$$

since under mutation-selection balance $p_l = \mu/s$ and U is defined $U := 2L\mu$, the deleterious mutation rate per diploid genome, per generation. They then set $V_A = V_{\text{BGS}}$, and note that $V_m \approx Us^2$, since mutations have frequency of $1/2N$ and each increase the variance by a factor of s^2 . Note that because the classic BGS model assumes deterministic selection dynamics (i.e. an infinite population), the equilibrium Z given by equation (38) excludes the reduction due to drift. The reduction factor under the strong BGS model is,

$$Z_{\text{BGS}} := 1 - \frac{V_m}{V_{\text{BGS}}} = 1 - \frac{Us^2}{Us} = 1 - s \quad (41)$$

(c.f. Santiago and Caballero 1998 equation 10). An alternate derivation can be found by working out the deterministic reduction in variance from the single-locus dynamics.

Now, we can use these values for Z_{BGS} , V_m , and V in equation (36). Through this alternate quantitative genetics derivation, we arrive at the same equation as classic BGS theory,

$$N_{d,\infty}^{\text{BGS}} = N \exp \left(-\frac{U}{2s + M - Ms} \right). \quad (42)$$

This matches equation 8 of Hudson and Kaplan (1995) except for the Ms term and equation 10 of Nordborg et al. (1996) except for the $2s$ term.

1.9 The Draft-Effective Population Size Under Weak and Strong BGS

With the possibility of weak selection, deleterious alleles can drift up in frequency and fix. Consequently, the fitness distribution is no longer stationary, as the set of haplotypes without any deleterious mutations can be lost due to drift. This changes the shape of the fitness distribution, and thus the variance parameter that our model relies upon (Gessler 1995; Good and Desai 2013; Haigh 1978; Higgs and Woodcock 1995; O’Fallon et al. 2010). So far, finding an explicit equation for the variance has been difficult due to the “moment-closure problem” previously mentioned. In their approximation, Santiago and Caballero (2016) consider a modified additive genic variance that is below V_{BGS} due to the loss of variation from each fixation of a weakly deleterious mutation. This fixation process is related to the Muller’s Ratchet, the rate R of fixation of deleterious mutations per generation per region, since each fixation directly reduces the additive genic variance of the fitness distribution. However, in general, the rate of this ratchet is unknown since it depends on the fitness variance (and thus higher moments of the fitness distribution).

In their 2016 paper, Santiago and Caballero derive use an approach based on Fisher’s Fundamental Theorem of Natural Selection (equation 2, Santiago and Caballero 2016, equation 15A Garcia-Dorado 2007). A more formal derivation follows from Higgs and Woodcock (1995) (though they assume a haploid asexual system, the end result is the same up to a factor of two). In their work, they derive equations for the change per generation for the moments and cross-moments of the fitness distribution under multiplicative selection in a haploid model. They find, the haploid rate of the ratchet is $r = u - sv_n$ (equation 13.3, Higgs and Woodcock 1995), where we use low-ercase to distinguish between haploid and diploid models. Here, v_n is the variance in the *number* of deleterious mutations; as long as selection is not too strong, the haploid additive variance is $v_A \approx s^2 v_n$. Substituting this for v_n and rearranging, the haploid fitness variance is related to the $v_A = us - rs$, which is identical to Santiago and Caballero’s (2016) equation 2, noting that the waiting time between fixations (i.e. ratchet clicks) is $T = 1/r$. Intuitively, the fitness variance $V_{\text{BGS}} = Us$ is reduced by the rate at which deleterious mutations fix and remove fitness variation from the population.

Now, note that under a diploid model, the fitness variance is twice that of the haploid model, so $V_A = 2v_A$. Then, the fitness variance is,

$$V_A = Us - 2Rs. \quad (43)$$

where $U = 2u$ and $R = r$ is the diploid rate of the ratchet, which depends on higher moments of the fitness distribution, but only differs from r through a rescaling of the population size. We also find that Equation (7) and Supplementary Materials Equation 43 above can also be found through Kimura’s diffusion models with a flux of mutations into infinite, discrete sites (1969). Note that if selected sites are sufficiently deleterious that they cannot fix (or the population is infinite), $R = 0$ and the additive fitness variance is identical to that under strong background selection, $V_A = Us = V_{\text{BGS}}$ (equation 40). We note that while we use V_A here following Santiago and Caballero (2016), this is only the *additive genic* component of additive fitness variation, as our simulations confirm in the main text.

Next, we turn to the fixation probability of a new deleterious mutation with additive effects ($1 - s$ in the heterozygote, $1 - 2s$ in the homozygote). In a diploid population with drift-effective population size N_e this is,

$$p_{\text{fix}} := \frac{1 - \exp(2N_e s/N)}{1 - \exp(4N_e s)} \approx \frac{2N_e s}{N(\exp(4N_e s) - 1)} \quad (44)$$

(c.f. Durrett 2008, equation 7.21; Kimura 1957, equation 5.6). Then, Santiago and Caballero argue that the rate of the ratchet is the inverse of the averaging waiting time until a fixation, $T \approx 1/(UNp_{\text{fix}})$ (note that since U is the *diploid* mutation rate, the total population mutation rate is UN per generation), so

$$T \approx \frac{\exp(4N_e s) - 1}{2UsN_e}. \quad (45)$$

Since the ratchet rate depends on N_e , which in turn depends on the rate of the ratchet, we write the ratchet, or substitution, rate per L -basepair region per generation as,

$$R(N_e) := \frac{2UsN_e}{\exp(4N_e s) - 1}. \quad (46)$$

Under weak and strong background selection the variance input of mutations V_m is the same, and using the V_A derived above, the decay in variance is

$$Z_{\text{WS}} = 1 - \frac{V_m}{V_A} = 1 - \frac{Us^2}{(U - R(N_e))s} = 1 - \frac{Us}{U - R(N_e)}. \quad (47)$$

At equilibrium, the N_e that determines fixation probability is the asymptotic $N_{d,\infty}$. Consequently, Santiago and Caballero argue that the asymptotic reduction in draft-effective population size uses the Q_∞^2 and is given by the following system of non-linear equations,

$$R(N_{d,\infty}) = \frac{4UsN_{d,\infty}}{\exp(4N_{d,\infty}s) - 1} \quad (48)$$

$$N_{d,\infty} \approx N \exp \left(-\frac{V_A}{(1 - Z)(2 - (2 - M)Z)} \right) \quad (49)$$

The solution to these equations is the asymptotic equilibrium \tilde{N}_d and equilibrium ratchet rate \tilde{R} . This sets the equilibrium variance, $\tilde{V} = Us - 2\tilde{R}s$, or $\tilde{V} = (U - 2\tilde{R})s$. Note that because $p_{\text{fix}} < 1/2N$ for deleterious variation, $2R < U$, or the diploid mutation rate must be greater than or equal to twice the per-basepair per-generation substitution rate for equilibrium variance $\tilde{V} > 0$ for $s > 0$.

2 Statistical Methods

2.1 Parametric Forms of Negative Linked Selection Models

Both classic BGS and the B' method we build off the SC16 model have the same parametric form, since both (1) model the impact of linked selection as a rescaling of effective population size, and (2) both assume multiplicative fitness across segments. Thus, the total reduction experienced by a neutral site at position x due to segments across the genome is the product of the individual reductions is

$$B(x, \Psi) = \prod_g^S \exp \left(\int_0^1 b(\mu(s, k(g)), s, L_g, r_g, d(x, g)) ds \right) \quad (50)$$

$$= \exp \left(\sum_g^S \int_0^1 b(\mu(s, k(g)), s, L_g, r_g, d(x, g)) ds \right) \quad (51)$$

where, $b(\mu(s, k(g)), s, L_g, r_g, d(x, g))$ is the log reduction due to segment g , and there are S total segments. Here, $\mu(s, k(g))$ is the per-basepair per-genome rate that mutations with selection coefficient s enter segments with feature class $k(g)$ (e.g. it incorporates the distribution of fitness effects and mutation rate), L_g and r_g are the length in basepairs and recombination rate per basepair

of segment g , and the recombination distance between focal site x and segment g is $d(x, g)$. The functional form of b varies depending on whether the classic BGS model is used (Supplementary Section 2.1.1), or our form of Santiago and Caballero’s (2016) equations (see Supplementary Section 2.1.2).

Under both background selection models used in our likelihood, the diversity in window v is $\bar{\pi}(v, \Psi) = \bar{B}(v, \Psi)\pi_0$. Here, $\bar{B}(v|\Psi)$ is the predicted reduction in diversity due to BGS in window v , given background selection parameters Ψ . In practice, we pre-calculate $B(x|\Psi)$ at fixed sites x across the genome, and take the average of the fixed sites B values within window v for the average $\bar{B}(v|\Psi)$.

2.1.1 Reductions Under the Classic BGS Model

The classic BGS model, which assumes deleterious mutations cannot fix, expresses the reduction for a focal site in the middle of a segment (Hudson and Kaplan 1995; Hudson and Kaplan 1994; Nordborg et al. 1996); here we consider a focal site directly to an arbitrary side of a segment under a deleterious mutations, and extend the model to handle a focal segment arbitrarily far from the segment. To simplify notation, we will only consider a single feature class in this and the next section. Using our notation from equation (56), the log reduction under the classic mutation-selection-balance BGS model is,

$$b(\mu, s, L, r, 0) = - \int_0^L \frac{2\mu(l)}{s(1 + (1-s)r(l)/s)^2} dl \quad (52)$$

(c.f. Hudson and Kaplan 1995 equation 5), where $\mu(l)$ is the *haploid* per-basepair mutation rate at l and $r(l)$ is the recombination fraction between the focal site (at position 0) and basepair l . Assuming constant per-basepair recombination and mutation rates, $r(l) = r_{BP}l$ and $\mu(l) = \mu$, and

$$b(\mu, s, L, r_{BP}, 0) = - \frac{2\mu L}{s + (1-s)r_{BP}L} \quad (53)$$

(c.f. Hudson and Kaplan 1995 equation 8, where the factor of two difference is due to the position of the focal site). Often per-region rates are defined $U = 2\mu L$ and $M = r_{BP}L$ are the segment-wide mutation diploid mutation rates (mutations per diploid segment per generation) and recombination length (Morgans).

For computational efficiency, we adjust this model by setting $r(l) = d + r_{BP}l$, where d is the recombination fraction between the focal site x and the start of segment g . This allows us to pre-compute the local effects of the segment, and substitute in b as the focal site changes. This integral substitution has a closed form,

$$b(\mu, s, L, r_{BP}, d) = \frac{-2\mu L}{(d(1-s) + s)(s + (d + r_{BP}L)(1-s))} \quad (54)$$

and terms can be collected in powers of d and pre-computed for all segments for the grid of μ and s . Our implementation pre-computes these segment components, and computes the final

b value for an x and g by calculating the distance $d(x, g) = |M(x) - M(g)|$, where $M(x)$ is the cumulative recombination map length at position x in Morgans. Since $r(l)$ could vary by position, segments with differing recombination rates are split into segments of the same annotation class by their recombination rate. This has no effect on the calculation due to the multiplicative fitness, but ensures more accurate estimates of the reduction factor B .

2.1.2 Reduction Under the Modified Santiago and Caballero Model

Under Santiago and Caballero’s model, the correct effective population size to gauge reduction in heterozygosity or coalescent times is given by their equation 4 (Santiago and Caballero 2016). This equation considers how the inflation factor Q_t^2 that sets the draft-effective population size varies over t (c.f. Supplementary equation 37). This is because selective processes can lead to non-constant pairwise coalescent rates, which impact pairwise coalescent rates and thus the reduction factor. We experimented with calculating this full sum and integral approximations to it in our methods, but it seemed to make little difference in our application. Additionally, it was too costly to calculate computationally for genome-wide calculations of the B’ map. Instead, we solve for the asymptotic $\tilde{N}_{e,\infty}$ for each segment, and use that to calculate the log reduction factor under the SC16 model, b' .

Note that the asymptotic model above determines the reduction in effective population size experienced by a focal site in the middle of a L -basepair segment, but B maps require the reduction b' experienced by a focal site x at an arbitrary recombination distance apart. For each segment, we pre-compute the solution to the system of two equations, giving us V and Q_∞^2 , and then use these values in the equation (??),

$$b'(\mu, s, L, r, d) = -\frac{V}{2} \left(\frac{1}{(1 - (1 - d)Z)} \right)^2 \quad (55)$$

where $Z = 1 - Us/(U - \tilde{R})$ and $V = Us - 2\tilde{R}s$. TODO check d.

2.2 Discretization of Parameters and Annotation Feature Classes

In practice, to fit such a model, we must discretize both $\mu(s, k(g))$ and s in Equation (56). We define μ_i to be the rate of mutations entering the population per basepair, per generation with selection coefficient s_i (i.e. the product of the mutation rate and the distribution of deleterious fitness effects). Then, the reduction at position x is,

$$B(x, \Psi) = \exp \left(\sum_g^S \sum_i b \left(\mu_{i, k(g)}, s_i, L_g, r_g, d(x, g) \right) \right). \quad (56)$$

Because it is computationally-intensive to numerically solve the system of two non-linear equations to calculate b at each segment, these are pre-computed for an m_s -element grid of selection coefficients and an m_μ -element grid of mutation rates–DFE products. The number of annotation features K is variable and set by the annotation data specified. There are two ways to parameterize the mutation rates and DFE for all annotation classes in background selection models. First, for the

free-mutation parameterization, each annotation feature class has a free mutation rate parameter for each of these selection coefficients (as in equation (56)).

In the free-mutation parameterization, there are $1 + K \times m_s$ for π_0 and the free mutation rate parameters, where K is the number of annotation features. The MLE optimization for this approach is unconstrained, though π_0 is bounded to be within $10^{-5} \leq \pi_0 \leq 10^{-1}$ and mutation rates are bounded within $10^{-11} \leq \mu \leq 10^{-7}$. The BGS model requires a mutation rate for each selection coefficient in the grid, for each annotation class (here, as an example, CDS, UTRs, and phastcons), which are stored in the $m_s \times K$ matrix \mathbf{M}_F ,

$$\mathbf{M}_F = \begin{bmatrix} \mu_{10^{-6},\text{CDS}} & \mu_{10^{-6},\text{UTR}} & \mu_{10^{-6},\text{PC}} \\ \mu_{10^{-5},\text{CDS}} & \mu_{10^{-5},\text{UTR}} & \mu_{10^{-5},\text{PC}} \\ \vdots & \vdots & \vdots \\ \mu_{10^{-1},\text{CDS}} & \mu_{10^{-1},\text{UTR}} & \mu_{10^{-1},\text{PC}} \end{bmatrix} \quad (57)$$

That is, the distribution of fitness effect (DFE) is implied by the total mutation rate across selection coefficients for an annotation class. We can normalize by the total mutation rate estimate to get the estimated DFE, giving us the DFE weight for annotation class k and selection coefficient with index i ,

$$\hat{w}_{i,k} = \frac{\hat{\mu}_{i,k}}{\sum_i \hat{\mu}_{i,k}}. \quad (58)$$

The second parametrization is the *simplex* parametrization, which has a single mutation rate across all features, so it is a DFE weight matrix times the mutation rate μ ,

$$\mathbf{M}_S = \mu \begin{bmatrix} w_{10^{-6},\text{CDS}} & w_{10^{-6},\text{UTR}} & w_{10^{-6},\text{PC}} \\ w_{10^{-5},\text{CDS}} & w_{10^{-5},\text{UTR}} & w_{10^{-5},\text{PC}} \\ \vdots & \vdots & \vdots \\ w_{10^{-1},\text{CDS}} & w_{10^{-1},\text{UTR}} & w_{10^{-1},\text{PC}} \end{bmatrix} \quad (59)$$

which has $2 + K \times (m_s - 1)$ free parameters, since each column must sum to one. This imposes the constraint that $\sum_i w_{i,k} = 1$, requiring constrained MLE optimization.

2.3 Data Summary Matrices

Our underlying data for all likelihood and pairwise diversity estimates is the allele count matrix \mathbf{C} with dimensions $L \times 2$, where L is the chromosome length. This is transformed to a pairwise summary matrix with identical dimensions, \mathbf{Y} . The first column of \mathbf{Y} is the number of pairwise comparisons between chromosomes that are identical, and the second column is the number that are different. Both of these columns are combinatoric summaries of the raw allele counts matrix needed for the binomial likelihood and pairwise diversity estimates. Let $[c_1, c_2]$ be a row of \mathbf{C} for basepair l (the l index is omitted for clarity), and $n = c_1 + c_2$. Then, the (1) total number of pairwise combinations of chromosomes n_T , (2) the number of pairwise with identical alleles n_S , and (3) the number of pairwise combinations with differing alleles n_D are respectively,

$$\begin{aligned}
n_T &= \frac{n(n-1)}{2} \\
n_S &= \binom{c_1}{2} + \binom{c_2}{2} \\
n_D &= n_T - n_S
\end{aligned}$$

which would be stored in row $\mathbf{Y}_l = [n_S, n_D]$. Note that the per-site \mathbf{Y} handles non-polymorphic sites and missing data. Non-polymorphic sites have $n_S = \binom{n}{2}$ and $n_D = 0$, and missing data has $n_S = n_D = 0$.

2.4 Pairwise Diversity Estimates

The pairwise diversity at site l across the n sampled chromosomes can be calculated from row l of the \mathbf{Y} matrix as follows,

$$\pi_l = \frac{n_D}{n_T} \quad (60)$$

which is identical to the more common expression of this estimator,

$$\pi_l = \frac{2}{n(n-1)} \sum_{i < j}^n k_{i,j} \quad (61)$$

where $k_{i,j}$ is 1 if the alleles at this site differ at site l , and 0 otherwise.

There are three ways to aggregate π_l across all sites. The first is,

$$\pi^{(1)} = \frac{1}{L} \sum_{i=1}^L \frac{n_{D,i}}{n_{T,i}} \quad (62)$$

which if the number of samples across loci is constant, simplifies to an unweighted average across sites. Second, one can take a weighted average, with weights determined by the total number of samples present at a site,

$$\pi^{(2)} = \frac{1}{\sum_{i=1}^L n_i} \sum_{i=1}^L n_i \frac{n_{D,i}}{n_{T,i}} \quad (63)$$

Third, one can weight by the number of pairwise comparisons at a site, $n_{T,i}$, rather than total number of samples, n_i , which leads to a ratio of sums,

$$\pi^{(3)} = \frac{\sum_{i=1}^L n_{D,i}}{\sum_{i=1}^L n_{T,i}}. \quad (64)$$

We predominantly use the estimator $\pi^{(3)}$, as it corresponds to how we summarize the matrix \mathbf{Y} across windows for our likelihood. All methods have mean squared errors and biases very close to one another (TODO).

Note, however, that estimates of pairwise diversity often condition on the accessible bases, and thus treat this as fixed. However, the number of accessible bases varies across the chromosome; this can lead to a source of apparent bias during block-bootstrap estimates of uncertainty. In this case, pairwise diversity is a ratio estimator, and is thus biased, since by Jensen’s inequality $\mathbb{E}(y/x) \geq \mathbb{E}(y)/\mathbb{E}(x)$ for random variables x and y .

2.5 Window-based Summaries and filtering

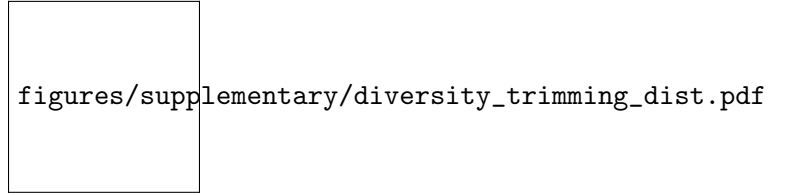


Figure 1: The distribution of diversity across the genome at the megabase scale, with outliers trimmed. The blue line is the normal CDF, fit with MLE parameters XXX. The inset figure is the untrimmed data, with trimmed points shown in red.

The likelihood method is fit to non-overlapping binned summaries of the allele counts matrix. Based on exploratory data analyses, some bins were outliers and excluded (XXX).

1. **Fraction of inaccessible sites per window.** `mask_inaccessible_bins_frac`
2. **Outliers:** Based on exploratory analysis, there were some regions with very high diversity. The 0.05% right tail was excluded.

2.6 Annotation Models

CADD 6%: 6.49% of autosomal sequence. CADD 8%: 8.56% of autosomal sequence.

2.7 Ratchet Rate Prediction

After rescaling each segment N_e by the local predicted reduction $\hat{B}(x)$, the ratchet rates and B' values are re-calculated.

The rescaled B' calculation outputs a $m_\mu \times m_s \times S$ multidimensional array \mathbf{R} of ratchet rates per segment. These are rescaled by the segment lengths \mathbf{L} , giving the per-basepair mutation rate array. The per-basepair ratchet rate given maximum likelihood estimates of $\hat{\mu}$ and $\widehat{\mathbf{W}}$ is used to predicted the ratchet rate for each segment g . The DFE estimate for feature k is a column vector of $\widehat{\mathbf{W}}$, i.e. $\widehat{\mathbf{w}}_k$

$$\lambda_D(g) = \tag{65}$$

The predicted ratchet rate for segment g $\lambda_d(g)$ is based on these values.

2.8 Numeric Optimization

mu bounds

bounds and time, bounds and convergence

Same optima, but took longer

2.9 Numeric methods for calculating B

Depending on the number of features, this can be incredibly memory intensive.

2.10 Optimization

Optimization in non-linear regression is notoriously difficult both in general (Bates) and in the specific problem of estimating the effects of genome-wide selection (Murphy et al. 2022). We experimented with a variety of global and local optimization approaches and parameterizations, but found that

3 Human Genomic Data

3.1

In order to try to ensure accurate estimation of pairwise diversity, which is a ratio estimator that is sensitivity to its denominator, we use the complete per-basepair genotype calls (gVCF) produced by Illumina’s DRAGEN pipeline (Illumina, Inc. 2020). The original samples were from 178 Yoruban individuals sequenced to 30x by the New York Genome Center (Byrska-Bishop et al. 2022). This allows for filtering to be applied to the entire genome at once, rather than just variants, so the denominator does not need to be estimated separately.

The full list of samples is available in TSV format in the GitHub repository (`data/h1kg/yri_samples.tsv`).

3.2 Filtering gVCFs

gVCFs were filtered using a custom Python tool, `gvcf2counts.py` (in `tools/gvcf2counts.py`), which reads the gVCFs, filters them according to the criteria below, and outputs a Numpy `.npy` file of reference and alternative allele counts for each chromosome (hereafter, “allele counts matrices”).

Genotypes are included in the allele count if and only if:

1. The variant call is set to `PASS` in the VCF.
2. The `QUAL > 50`.
3. The `GQ > 30` (or `RGQ > 30` for invariant sites).

Because the data underlying the counts files are per-basepair resolution gVCFs, each chromosome’s allele counts matrix is of size $l \times 2$, where l is the total chromosome length. Basepairs that fail these filtering requirements lead to a row of zero counts, e.g. no observed reference and alternative allele counts, and thus do not effect the data that goes into the binomial likelihood or π estimates used in figures.

3.3 Non-accessible and Masked Regions

The allele counts matrices include many basepairs that may have allele counts that pass the genotype call filters, but are still need to be filtered out because the region of the genome may produce unreliable estimates. The following filters are applied based on masking regions:

1. **Non-accessible regions:** masks out centromeres (`acen` entries in `cytoBand.txt`), with 5Mbp padding on either side. The file of passing masks is `data/annotation/no_centro.bed`.
2. **Reference masking:** soft and hard-masked regions in the human GRCh38 reference genome are also masked. Soft-masked regions were determined by Ensembl (XXX), which uses Repeat Masker (XXX) and Dust (XXX). Additionally, we used the 1000 Genomes strict filter (XXX).

3.4 Putatively Neutral Tracks

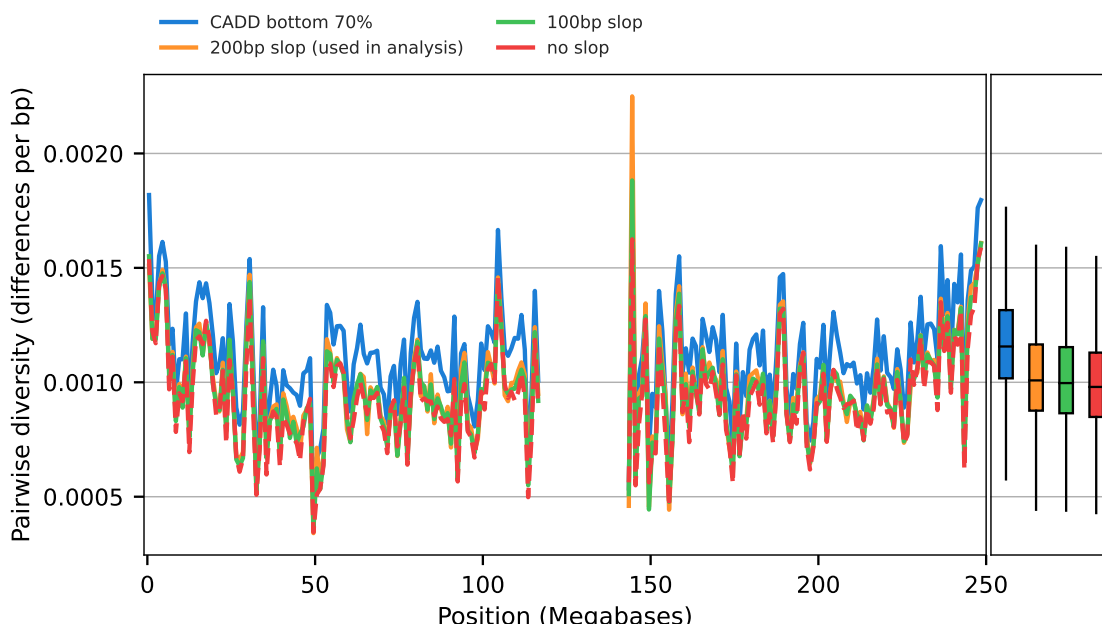


Figure 2: Estimates of chromosome 1 YRI diversity in non-overlapping megabase windows, under different neutral tracks (colors) and the filtering criteria described in Supplementary Section 3.3. To the right of the chromosome subfigure are the genome-wide boxplots of megabase-scale diversity.

Linked selection theory typically assumes that focal sites are not under purifying selection themselves. Consequently, linked selection statistical methods often only consider the fraction of the genome not *a priori* under selective constraint (Murphy et al. 2022, e.g. Appendix Section 3.1). Our methods follow suit, and first create a track consisting of the union (i.e. `bedtools merge`) of: exons and coding sequences from Ensembl Version 107 (Cunningham et al. 2022, `Homo_sapiens.GRCh38.107.chr.gff3.gz`) and PhastCons regions (Siepel et al. 2005, `phastConsElements100way.bed.gz`). Then, we remove 200 basepairs of “slop” around each of these regions (i.e. `bedtools slop`). We show in Supplementary Figure 2 that average diversity (we only consider YRI samples for this analysis) is fairly insensitive to the slop width, but increasing slop widths around putatively

conserved segments does lead to higher diversity estimates. This is expected, since increasing the slop width considers a smaller subset of sites, further away from putatively conserved regions. For our analyses we choose the 200bp slop version, which covers 63.66% of the autosomal reference sequence and consists of 1.26 million contiguous genomic regions.

Additionally, we compared our neutral track (and the slop width alternatives) against the bottom 70% of CADD site scores (this works out to be 64.70% of the autosomal reference sequence). The correlation between these two tracks is extraordinarily high (Pearson $r = 0.98$, p-value = 0), but the average pairwise diversity is 13% higher (two-tailed t-test p-value 1.29×10^{-71}) in the CADD bottom 70% neutral track. However, we did not use the CADD bottom 70% neutral track in our analysis of human population genomic data. Our concern was that because CADD models are trained by differentiating high-frequency derived SNPs in humans from simulated variants at every basepair, there could be circularity in basing our neutral regions on predictions based on modeling frequency data. Moreover, this neutral track would be close to a complement of the CADD 6% track, which we use as one of our annotation models, and might lead to issues. Additionally, the CADD bottom 70% neutral track is much less sparse than the track we used in our analysis, with a total of ≈ 20 times more contiguous regions than the neutral track used in analysis (25.38 million total). Many of these ranges are at very small spatial scales (average: ≈ 7 basepairs).

Additionally, we ran one test model with the CADD bottom 70% as the neutral track as a test. Using the CADD bottom 70% neutral track with the CADD 6% annotation model, the in-sample was $R^2 = 63.99\%$; by comparison, the in-sample $R^2 = 68.03\%$ using the constructed neutral track with 200bp slop. Overall, future work calibrating the neutral track is needed.

These neutral tracks are all produced by the Snakemake file `data/fit_annotation/Snakemakefile` in this study's GitHub repository (<http://github.com/vsbuffalo/bprime>).

3.5 Model Comparisons

3.6 Table of R^2 Values

3.7 Derivation of Approximate Drift R^2

Our approach models the observed megabase-scale diversity y_i in window i as the predicted level under our negative selection model, $\pi_0 B_i$, plus some random residual error ε_i ,

$$y_i = \pi_0 B_i + \varepsilon_i \quad (66)$$

where each $B_i = f(X_i|\Psi)$ for some data X_i (i.e. the recombination map and annotation model) and parameters Ψ . To compare our models and assess model goodness-of-fit, we use the out-sample R_{LOO}^2 which is calculated by fitting the genome-wide model leaving one chromosome out, and calculating the residual variance between predictions and observed values for this out-sample chromosome.

In general, R^2 is calculated for a model fit across windows as,

$$R^2 = 1 - \frac{V_{\text{res}}}{V_{\text{tot}}} \quad (67)$$

where V_{res} is the mean squared error across windows and V_{tot} is the total variance in the predictor. Suppose we have estimates $\hat{\pi}_0 \hat{B}_i$ for $\pi_0 B_i$ from our model. Then,

Table 1: Percent of basepairs remaining that are accessible and putatively neutral.

Chromosome	Accessible	Neutral	Intersection
chr1	39.7	61.2	23.4
chr2	45.3	67.3	27.5
chr3	43.2	67.3	25.7
chr4	42.7	70.5	27.4
chr5	42.4	67.5	26.0
chr6	43.8	67.9	26.7
chr7	41.9	67.8	26.2
chr8	42.3	70.9	27.5
chr9	36.2	58.1	22.0
chr10	42.9	68.2	26.8
chr11	41.3	67.0	25.0
chr12	40.6	67.2	24.1
chr13	38.8	59.8	25.2
chr14	36.5	54.9	21.5
chr15	34.4	53.7	20.6
chr16	36.0	62.5	23.1
chr17	37.2	63.3	21.6
chr18	40.3	65.7	26.3
chr19	28.1	66.1	17.0
chr20	36.1	65.1	22.4
chr21	29.8	55.9	20.9
chr22	25.5	50.9	17.1

Table 2: R^2 and mutation rate estimates for all models. XXX note about repeats

Model	Track type	Pop.	B' R^2_{LOO}	B' R^2_{IS}	B R^2_{IS}	B' $\hat{\mu} \times 10^{-8}$	B $\hat{\mu} \times 10^{-8}$
phastcons>CDS>genes	sparse	YRI	68.45	68.16	65.23	1.8636	0.2975
phastcons>CDS>genes	full	YRI	68.19	68.12	63.67	1.7082	0.1666
CADD 6%	full	YRI	68.08	68.08	62.96	1.4612	0.1721
CADD 6%	sparse	YRI	68.04	68.03	68.01	2.0912	2.0716
CADD 8%	full	YRI	66.98	67.11	63.61	1.0126	0.1713
CADD 8%	sparse	YRI	66.67	67.01	66.98	1.5688	1.5473
CDS>genes>phastcons	full	YRI	64.90	65.51	61.23	4.1951	0.1620
CDS>genes>phastcons	sparse	YRI	64.90	65.51	63.16	4.1795	0.3070
phastcons>CDS>genes	sparse	CEU	61.98	63.02	60.02	2.0194	0.3036
phastcons>CDS>genes	full	CEU	61.78	63.01	58.57	2.3499	0.1679
CADD 6%	full	CEU	61.74	62.94	57.42	1.5365	0.1739
CADD 6%	sparse	CEU	61.66	62.86	62.84	2.1215	2.1084
CADD 8%	full	CEU	60.80	62.12	57.95	1.1572	0.1742
CADD 8%	sparse	CEU	60.59	62.06	62.04	1.6030	1.5876
CADD 6%	full	CHB	59.62	61.31	55.31	1.5083	0.1727
CADD 6%	sparse	CHB	59.54	61.21	61.20	2.1242	2.1170
phastcons>CDS>genes	sparse	CHB	59.44	61.08	57.88	2.1982	0.3060
phastcons>CDS>genes	full	CHB	59.29	61.08	56.71	2.5573	0.1694
CADD 8%	full	CHB	58.88	60.63	55.86	1.1128	0.1733
CADD 8%	sparse	CHB	58.65	60.57	60.55	1.6098	1.6001
CDS>genes>phastcons	sparse	CEU	58.58	60.30	58.41	4.1041	0.3110
CDS>genes>phastcons	full	CEU	58.58	60.30	56.75	4.1001	0.1648
CDS>genes>phastcons	sparse	CHB	56.48	58.73	56.60	3.7195	0.3136
CDS>genes>phastcons	full	CHB	56.48	58.73	54.95	3.7552	0.1654

$$V_{\text{res}} = \frac{1}{n} \sum_{i=1}^n (y_i - \hat{\pi}_0 \hat{B}_i)^2 \quad (68)$$

$$= \underbrace{\frac{1}{n} \sum_{i=1}^n \varepsilon_i^2}_{\text{irreducible error}} + \underbrace{\left(\frac{1}{n} \sum_{i=1}^n (\pi_0 B_i - \hat{\pi}_0 \hat{B}_i) \right)^2}_{\text{bias squared}}. \quad (69)$$

The total variance in the predictor is,

$$V_{\text{tot}} = V_{\text{res}} + V_{\text{model}} + 2\hat{\pi}_0 \text{cov}_i(\varepsilon_i, \hat{B}_i) \quad (70)$$

where

$$V_{\text{model}} = \frac{\hat{\pi}_0^2}{n} \sum_{i=1}^n \left(\hat{B}_i - \frac{1}{n} \sum_{i=1}^n \hat{B}_i \right)^2. \quad (71)$$

Generally, fitting procedures act to minimize the squared deviation between predictors and observed values, which drives $\text{cov}_i(\varepsilon_i, \hat{B}_i)$ to zero XXX. Murphy et al. (2022) suggest XXX

Thus, our R^2 depends on (1) the bias of our predictors, (2) the covariance between residuals and predictors, and (3) the irreducible error due to variance in diversity within windows. However, it is of interest to approximate the irreducible error under theoretic models that assume all irreducible error is due entirely to the variance of coalescence times in a window, assuming that all of the effects of negative selection on the variance can be thought of as a local reduction in the effective population size to $B_i N_e$ and demographic effects amount to a simple rescaling of N_e . This also assumes mutation rates are constant across the genome, and do not contribute to the irreducible variance. We call this theoretic goodness-of-fit under drift R_{drift}^2 , and it provides a rough approximation of the irreducible error in our model due to “coalescence noise” around the modeled reductions due to negative selection.

Then,

$$\mathbb{E}(\varepsilon_i^2) = V(\pi_i) \quad (72)$$

since the mean residual is zero. The variance in pairwise diversity $V(\pi_i)$ is equivalent to the variance in the number of segregating sites for a sample of two, $V(\pi) = V(S_2)$. The variance in coalescence times in a window of width w basepairs with population-scaled recombination rate $\rho = 4B_i N_e r w$ is,

$$V(S_2) = \theta + \theta^2 \frac{2}{\rho^2} \int_0^\rho (\rho - x) f_2(x) dx \quad (73)$$

(Wakeley 2009, eq. 7.20) where,

$$f_2(\rho) = \frac{\rho + 18}{\rho^2 + 13\rho + 18}. \quad (74)$$

Since this is a rough approximation, we set $\theta = w\pi_0 B_i$ and fix $\rho = w\gamma\pi_0 B_i$ where γ is the ratio of recombination to mutation rates, r/μ . In humans, $\gamma \approx 1$, but we explore different ratios to assess sensitivity of this calculation (Supplementary Figure ??).

This back-of-the-envelope calculation finds that the upper bound of R^2 would be around 67% for Yoruba, and 64% for European and Han Chinese models (Figure 3). This rough approximation assumes constant demography, which for bottlenecked out-of-Africa populations assumes that the variance in coalescence times is determined entirely by reducing the effective population size. However, the variance in coalescence times is *higher* in bottlenecked populations (CEU and CHB) compared to Yoruba, which we confirm with simple simulations using the `OutOfAfrica_3G09` model from `stdpopsim` (Adrion et al. 2020; Gutenkunst et al. 2009). This higher than expected variance would inflate SS_{res} , which would decrease R^2_{drift} , bringing it closer to the observed R^2_{LOO} . A more accurate approximation of the R^2_{drift} could be found with simulations with more realistic demography and varying coalescence rates along the genome.

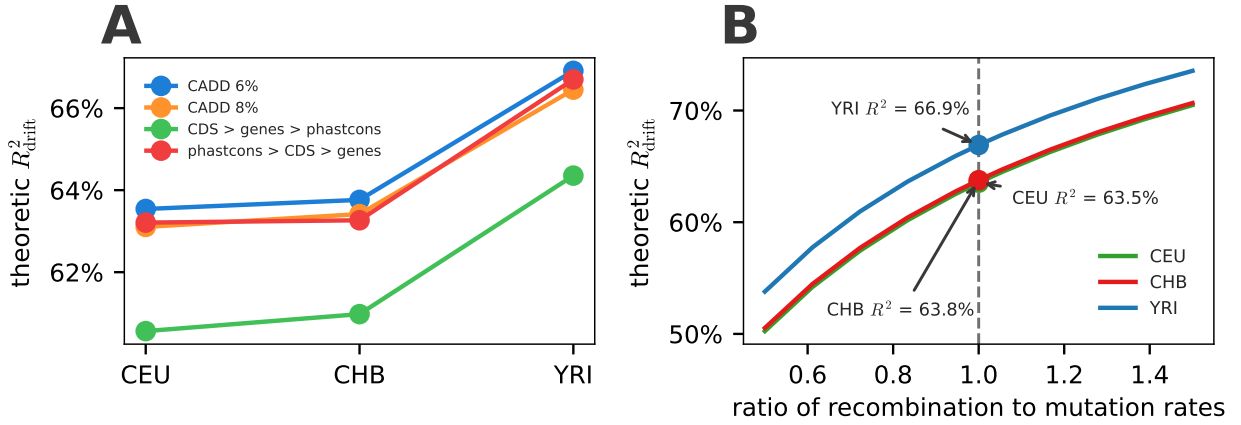


Figure 3: (A) the theoretic R^2_{drift} using different plugin estimators for B_i under different models. This shows that among the best-fitting models, the predicted R^2_{drift} varies little; most variation is among populations due to differing π_0 . (B) The R^2_{drift} across different populations, for varying ratio of recombination to mutation rates (x-axis).

3.8 Predicted Rate of Fitness Change

Each fixation of a mutant with fitness effect $-s$ reduces the population fitness to $1 - 2s$ since all individuals are homozygotes for the deleterious mutation and we assume additive effects at a site. For each segment l , the maximum likelihood parameter estimates of our model imply a prediction of the deleterious substitution rate per segment $\hat{R}_{l,i}$ for each selection coefficient s_i in the m_s -element DFE grid (according to which feature class it belongs to).

Since we assume multiplicative fitness effects, the log population fitness (considering only fixed sites) for segment l in the next generation is,

$$\log(L_l) = \sum_{i=1}^{m_s} \log(1 - 2s_i) \hat{R}_{l,i}. \quad (75)$$

Since we assume multiplicative fitness, the total genome-wide log population fitness in the next generation is

$$\log(L) = \sum_l \log L_l. \quad (76)$$

This amounts to a predicted population fitness loss per generation of

$$\begin{aligned} \hat{\Delta}_W &= 1 - L \\ &= 1 - \exp \left(\sum_l \sum_{i=1}^{m_s} \log(1 - 2s_i) \hat{R}_{l,i} \right). \end{aligned} \quad (77)$$

We calculate this value for all segments within a feature class, and then sum over all features to arrive at our genome-wide estimate. We use a parametric bootstrap to carry forward the estimation uncertainty to the predicted fitness loss per generation. Briefly, we do this by sampling new estimates of the DFE per selection coefficient and feature from a normal distribution centered on the ML point estimate and with the jackknife standard deviation.

3.9 Likelihood

Our model is essentially a generalized nonlinear model with a binomial link function. This is the form used by Elyashiv et al. (2016) and Murphy et al. (2022). These models fit the observed number of pairwise nucleotide differences in genomic windows to the expected pairwise diversity under some evolutionary model. We only consider BGS models here, so the mean function for position x is the product of the proportion by which BGS reduces diversity at position x , $B(x)$, and genome-wide neutral diversity π_0 ,

$$\pi(x) = B(x, \Phi) \pi_0 \quad (78)$$

Φ is the set of BGS parameters (i.e. the DFE for each feature type and mutation rate), and $\pi_0 = 4N_e\mu$ is determined by the genome-wide drift-effective population size N_e , set by only reproductive and demographic processes. Regional mutation rate heterogeneity can be accounted for with a regional mutation rate scaling function $m(x)$, $\pi(x) = B(x, \Phi)m(x)\pi_0$, but we do not explore mutation-rate heterogeneity, as it is unclear how to differentiate variance in mutation rate from the substitution rate heterogeneity we find across the genome.

The likelihood of the set of parameters $\Psi = \{\pi_0, \Phi\}$ can be written in the form of,

$$\log \mathcal{L}(\Psi) = \sum_{v \in \mathcal{V}} \sum_{i \neq j \in \mathcal{S}} \log(P(O_{i,j}(v) | \Psi)) \quad (79)$$

(c.f. Elyashiv et al. 2016; McVicker et al. 2009; Murphy et al. 2022) where \mathcal{V} is the set of putatively neutral sites, \mathcal{S} is the set of samples, and Ψ are the BGS parameters. The indicator variable $O_{i,j}(v)$ is 1 if samples i and j are different at putatively neutral site v , and zero otherwise.

While the theoretic $\pi(v)$ gives the average number of pairwise differences, for small values, this is approximately the heterozygosity probability, so we can write

$$P(O_{i,j}(v)|\Psi) = \begin{cases} \pi(v), & O_{i,j}(v, \Psi) = 1 \\ 1 - \pi(v), & O_{i,j}(v, \Psi) = 0 \end{cases}. \quad (80)$$

(c.f. Elyashiv et al. 2016).

As in Section 2.4, the number of pairwise differences and the total number of pairwise comparison at a site are sufficient statistics for the likelihood. Then, the binomial log-likelihood for the data at site v is,

$$\ell_v(\Psi) = \log(\pi(v, \Psi))n_{D,v} + \log(1 - \pi(v, \Psi))n_{S,v} \quad (81)$$

3.10 The scale of processes

We can observe $\hat{\pi}(x)$ at a per-basepair resolution. However, for a variety of reasons, we do not want to fit the composite likelihood model to the per-basepair scale of data. First, this would be computationally infeasible. Second, the mean function $\pi(x)$ varies on a natural scale that is itself a free parameter of the model. Our model can be written as,

$$\ell(\Psi, h) = \sum_b \sum_{v \in \mathcal{V}_b} \ell_v(\Psi) \quad (82)$$

$$= \sum_b \left[\log(\bar{\pi}(b, \Psi)) \sum_{v \in \mathcal{V}_b} n_{D,v} + \log(1 - \bar{\pi}(b, \Psi)) \sum_{v \in \mathcal{V}_b} n_{S,v} \right] \quad (83)$$

$$= \sum_b [\log(\bar{\pi}(b, \Psi))Y_{D,b} + \log(1 - \bar{\pi}(b, \Psi))Y_{S,b}] \quad (84)$$

$$(85)$$

where h is the bandwidth or window size, b the bin index for windows of width h , \mathcal{V}_b is the set of putatively neutral sites in bin b , $\bar{\pi}(b|\Psi)$ are the average diversity in bin b , and $Y_{S,b}$ and $Y_{D,b}$ are the sums across putatively neutral sites within a bin. Note that by binning, we sum the pairwise summaries of the data \mathbf{Y} across sites, so the likelihood across bins is naturally weighted by the quantity of observed data.

This model corresponds to a binomial likelihood for the observed data summarized at genomic scale h . Thus an alternative way to express this model is as,

$$Y_{D,b} \sim \text{Binom}(\bar{\pi}(b, \Psi), Y_{D,b} + Y_{S,b}). \quad (86)$$

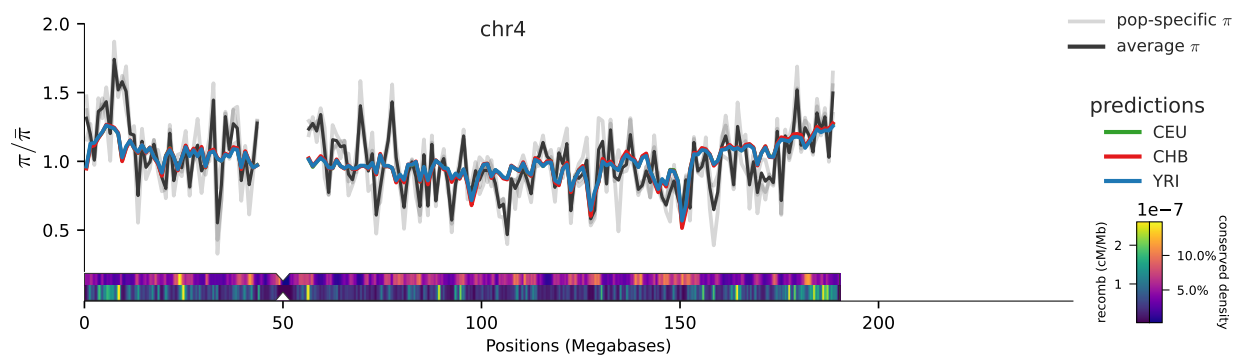
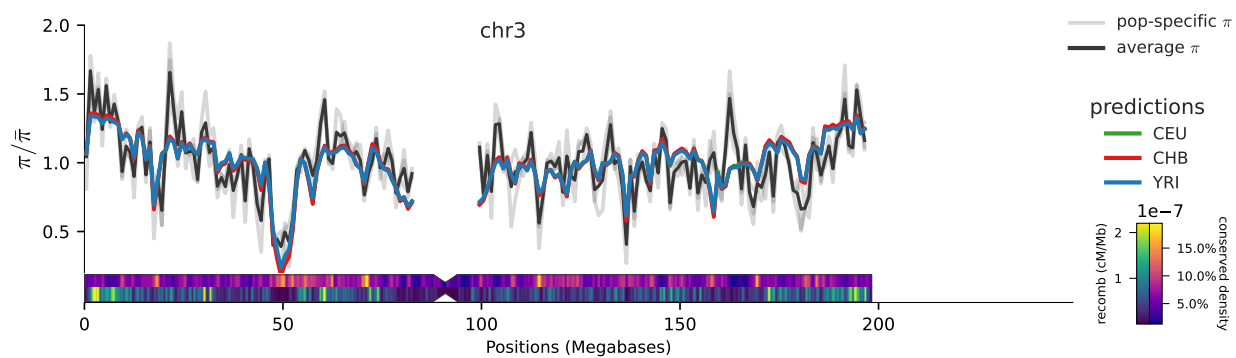
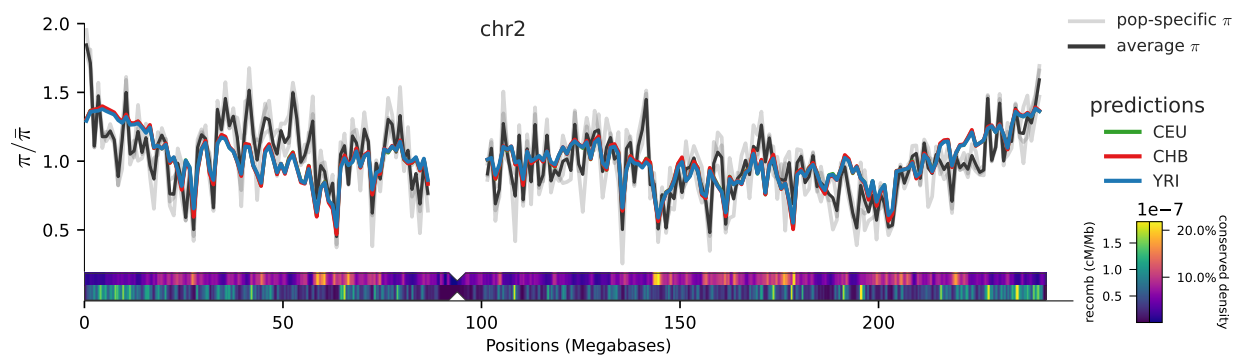
Here, $\bar{\pi}(b, \Psi)$ is assumed to be the *probability* of sampling two different alleles, rather than the average *number* of pairwise differences; these are approximately equal when π is small. This corresponds to an identity link function; one could alternatively use a two-alleles finite sites model link function of the form, $\pi/(1 + 2\pi)$. We experimented with this and found there was little difference between these link functions, so we opted for the simpler identity link function.

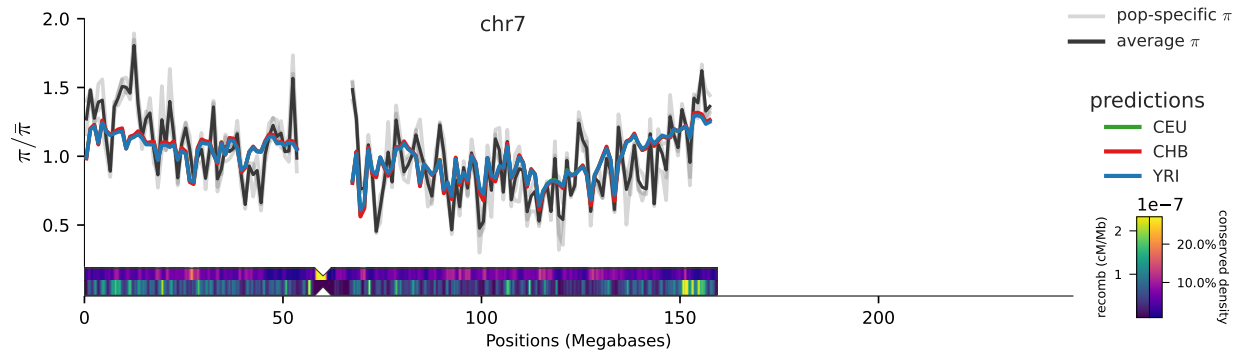
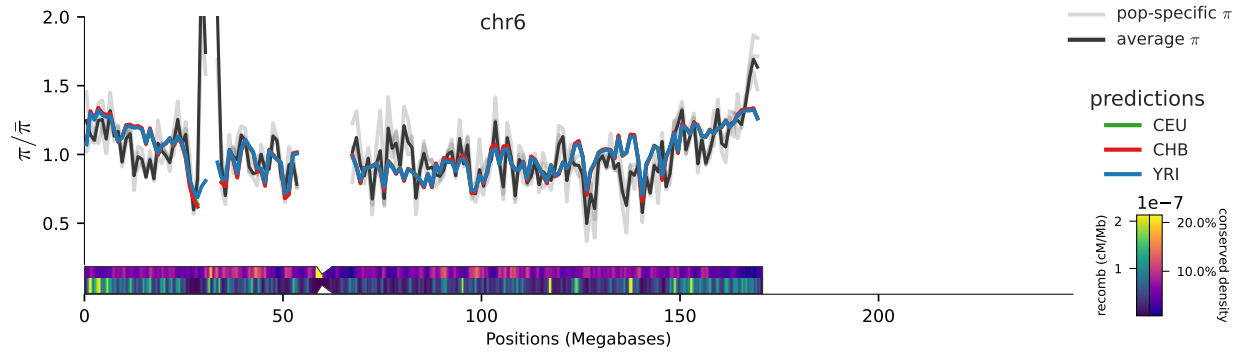
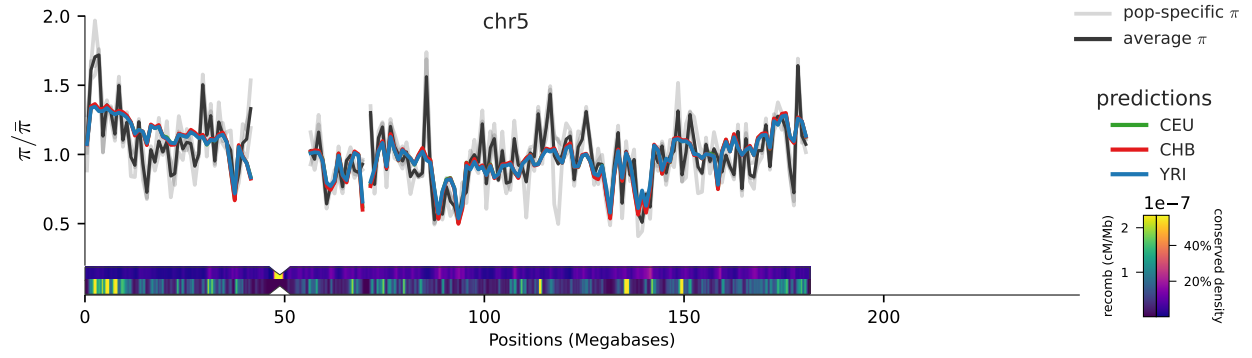
4 Simulations

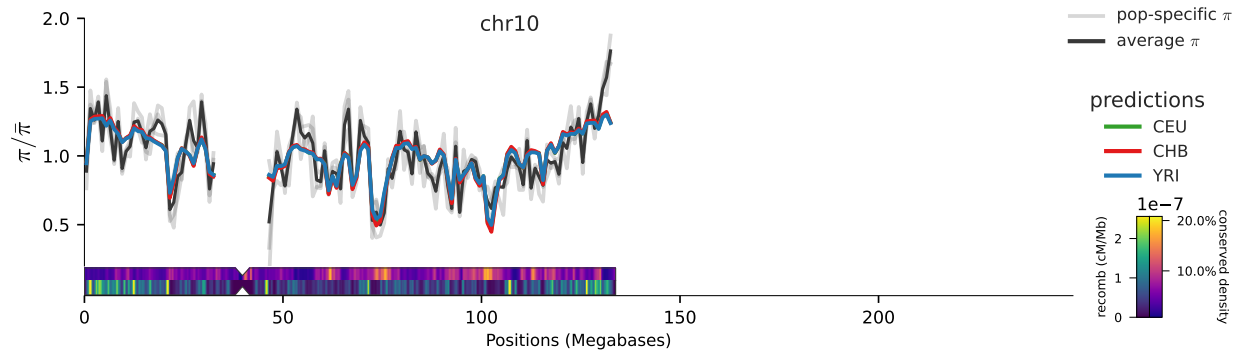
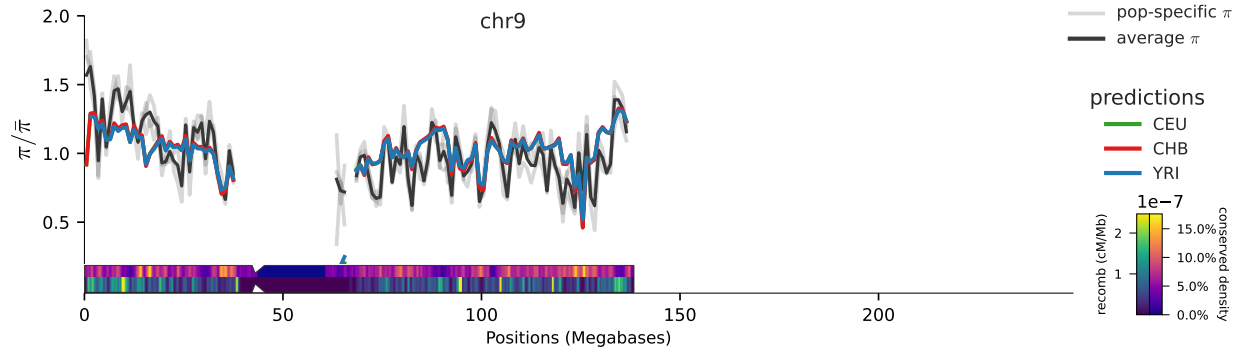
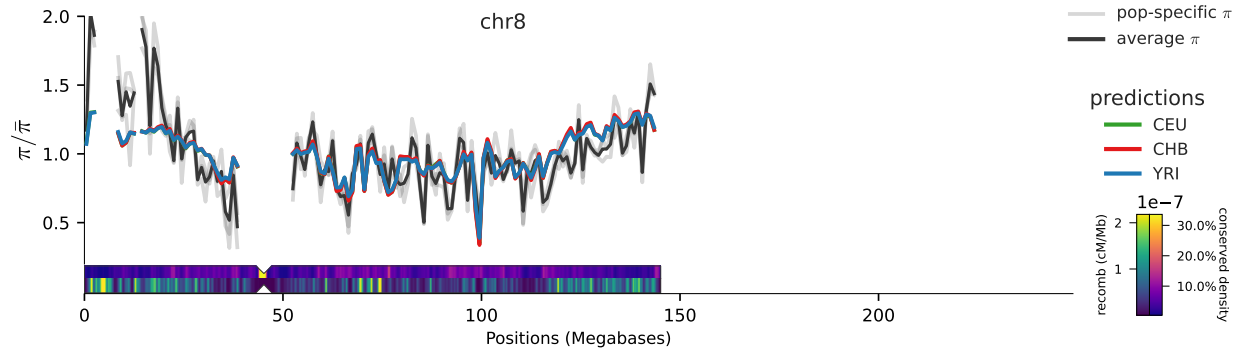
4.1 Segment Simulations

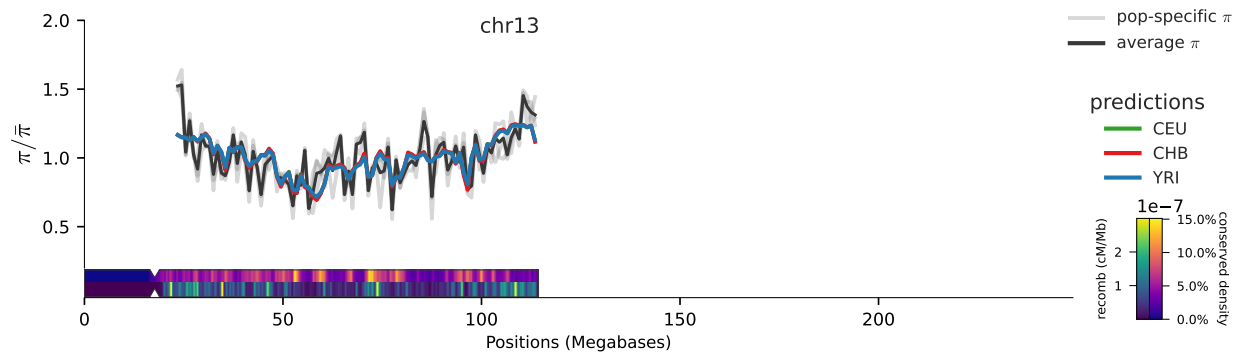
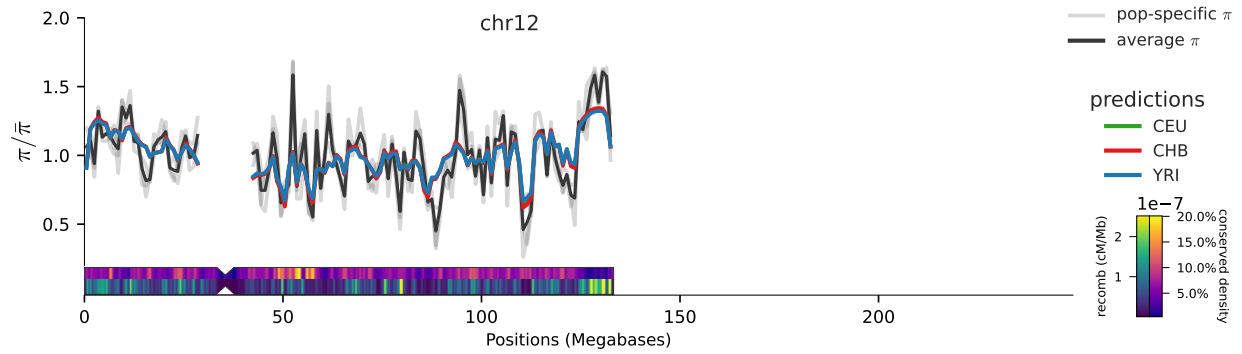
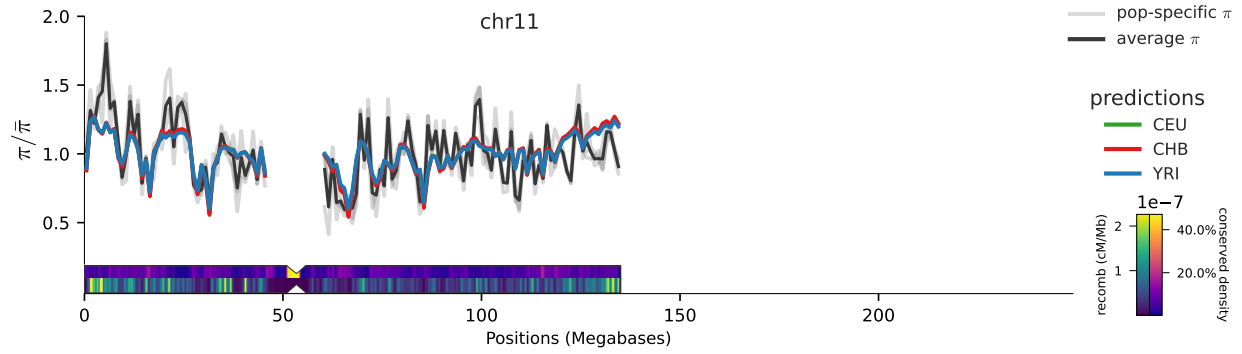
5 Additional Results and Figures

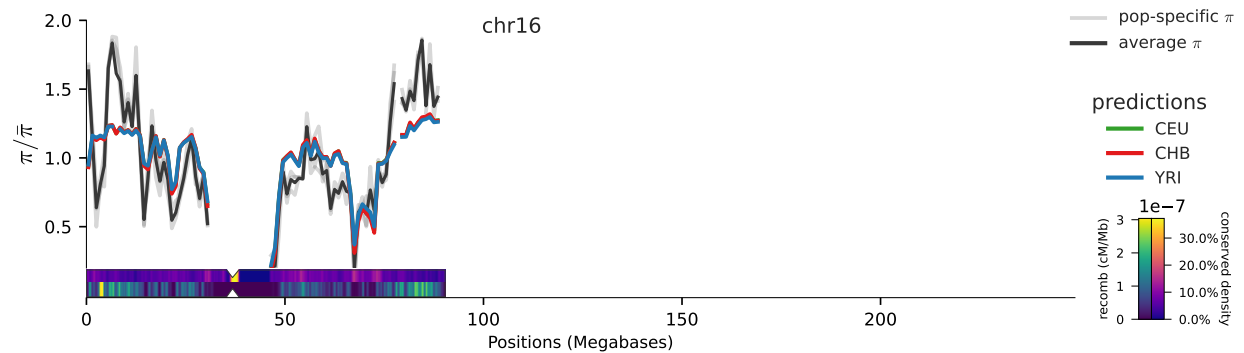
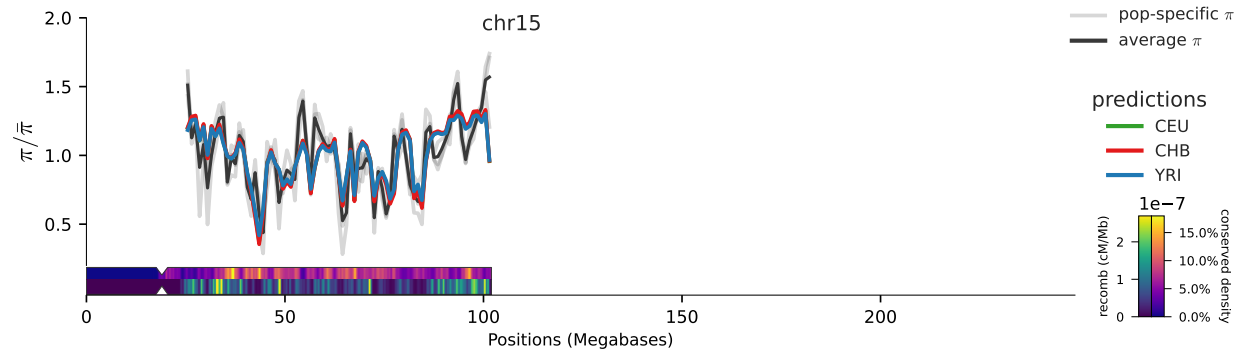
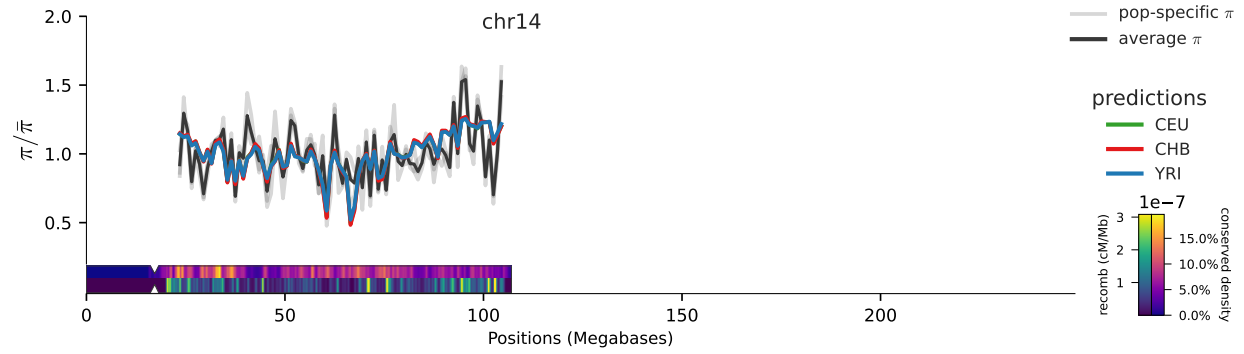
5.1 Chromosome Fit Figures

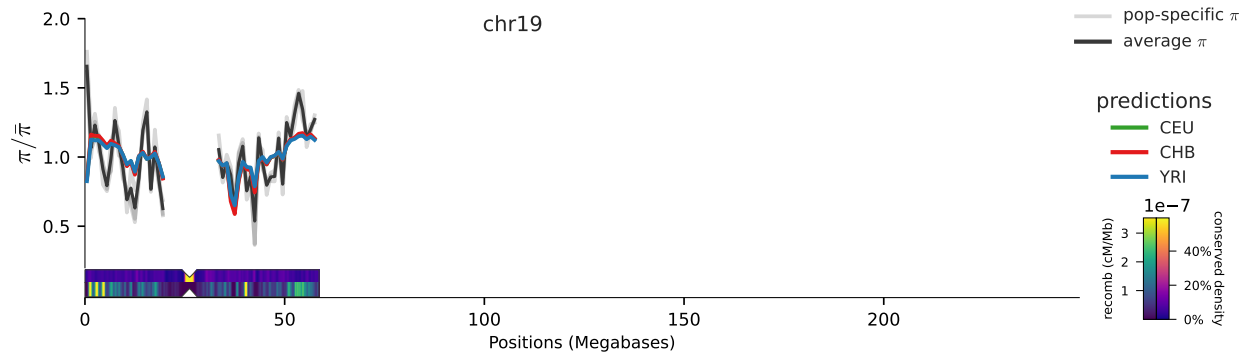
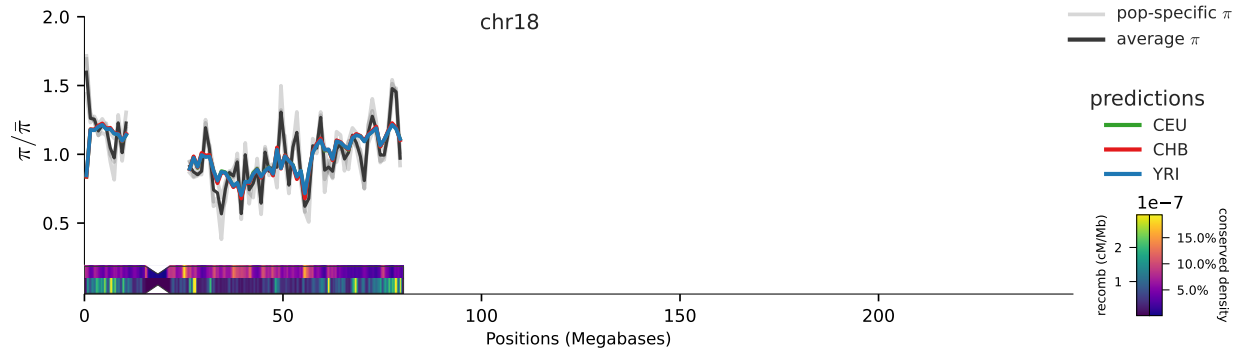
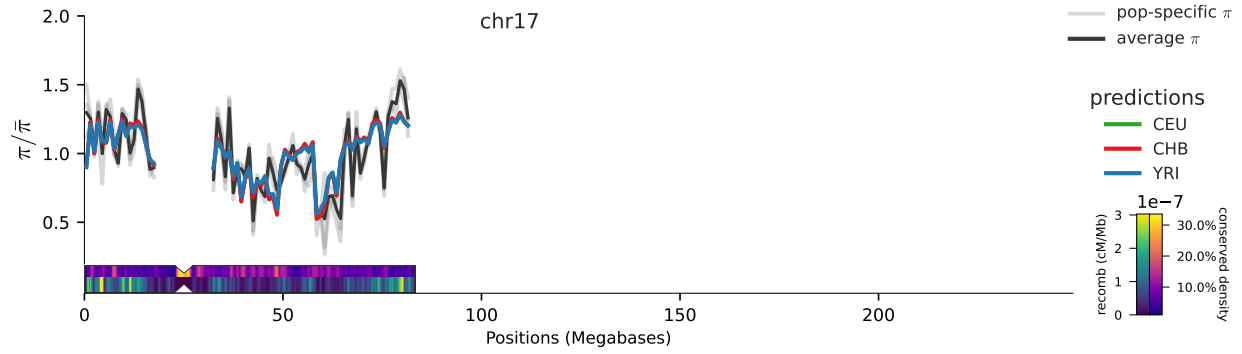


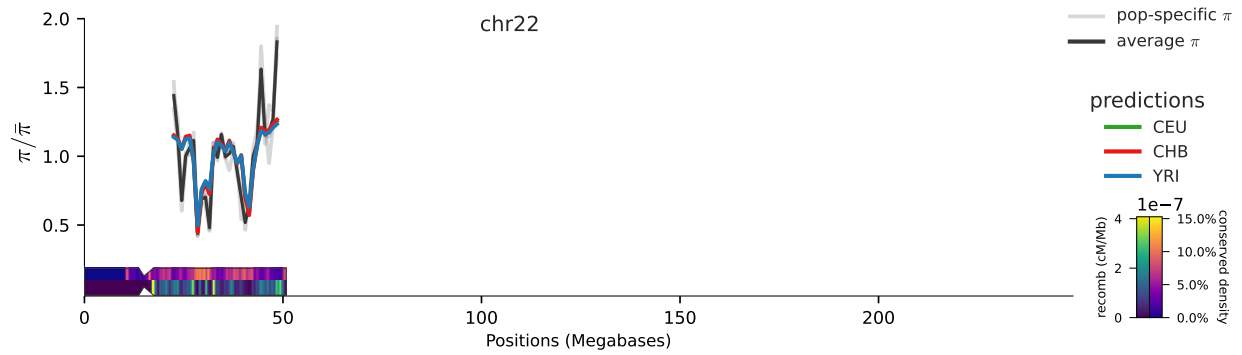
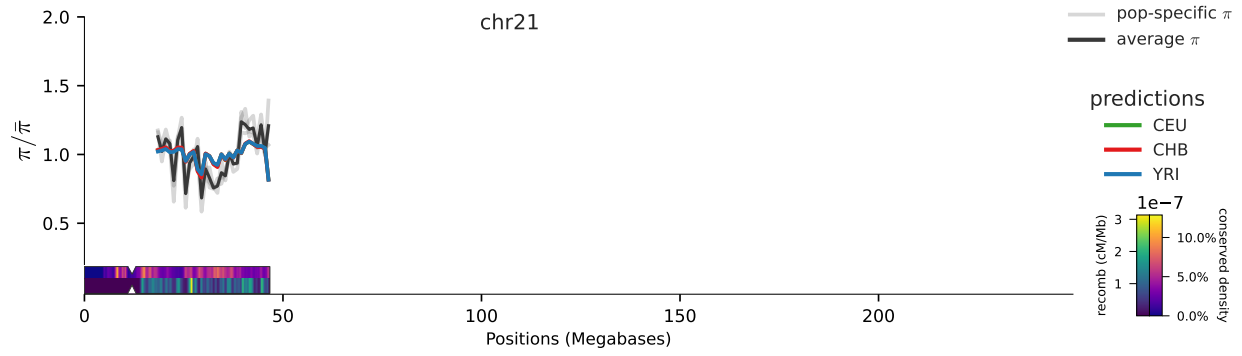
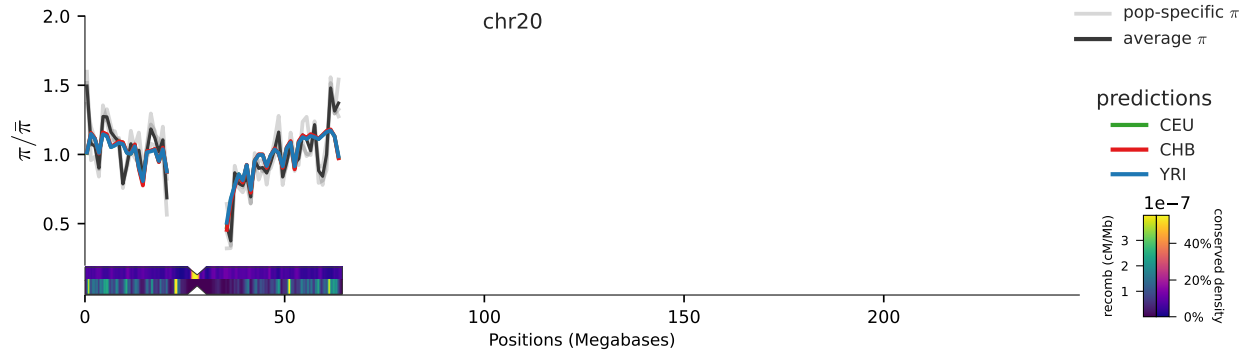












References

- Adrion, Jeffrey R et al. (2020). “A community-maintained standard library of population genetic models”. en. In: *Elife* 9.
- Barton, N H (1986). “The maintenance of polygenic variation through a balance between mutation and stabilizing selection”. In: *Genet. Res.* 47.3, pp. 209–216.
- (2000). “Genetic hitchhiking”. en. In: *Philos. Trans. R. Soc. Lond. B Biol. Sci.* 355.1403, pp. 1553–1562.
- Buffalo, Vince and Graham Coop (2019). “The Linked Selection Signature of Rapid Adaptation in Temporal Genomic Data”. en. In: *Genetics* 213.3, pp. 1007–1045.
- Byrska-Bishop, Marta et al. (2022). “High-coverage whole-genome sequencing of the expanded 1000 Genomes Project cohort including 602 trios”. en. In: *Cell* 185.18, 3426–3440.e19.
- Charlesworth, B (1987). *The heritability of fitness*. Sexual selection: testing the alternatives.
- Crow, James F (1958). “Some possibilities for measuring selection intensities in man”. en. In: *Hum. Biol.* 30.1, pp. 1–13.
- Cunningham, Fiona et al. (2022). “Ensembl 2022”. en. In: *Nucleic Acids Res.* 50.D1, pp. D988–D995.
- Durrett, Richard (2008). *Probability models for DNA sequence evolution*. Springer Science & Business Media.
- Elyashiv, Eyal et al. (2016). “A Genomic Map of the Effects of Linked Selection in *Drosophila*”. en. In: *PLoS Genet.* 12.8, e1006130.
- Garcia-Dorado, Aurora (2007). “Shortcut predictions for fitness properties at the mutation-selection-drift balance and for its buildup after size reduction under different management strategies”. en. In: *Genetics* 176.2, pp. 983–997.
- Gessler, D D (1995). “The constraints of finite size in asexual populations and the rate of the ratchet”. en. In: *Genet. Res.* 66.3, pp. 241–253.
- Good, Benjamin H and Michael M Desai (2013). “Fluctuations in fitness distributions and the effects of weak linked selection on sequence evolution”. en. In: *Theor. Popul. Biol.* 85, pp. 86–102.
- Gutenkunst, Ryan N, Ryan D Hernandez, Scott H Williamson, and Carlos D Bustamante (2009). “Inferring the joint demographic history of multiple populations from multidimensional SNP frequency data”. en. In: *PLoS Genet.* 5.10, e1000695.
- Haigh, John (1978). “The accumulation of deleterious genes in a population—Muller’s Ratchet”. In: *Theor. Popul. Biol.* 14.2, pp. 251–267.
- Higgs, Paul G and Glenn Woodcock (1995). “The accumulation of mutations in asexual populations and the structure of genealogical trees in the presence of selection”. In: *J. Math. Biol.* 33.7, pp. 677–702.
- Houle, D (1992). “Comparing evolvability and variability of quantitative traits”. In: *Genetics*.
- Hudson, R R and N L Kaplan (1995). “Deleterious background selection with recombination”. en. In: *Genetics* 141.4, pp. 1605–1617.
- Hudson, Richard R and Norman L Kaplan (1994). “Gene Trees with Background Selection”. In: *Non-Neutral Evolution: Theories and Molecular Data*. Ed. by Brian Golding. Boston, MA: Springer US, pp. 140–153.
- Illumina, Inc. (2020). *1000 Genomes Phase 3 Reanalysis with DRAGEN 3.5 and 3.7*. <https://registry.opendata.aws/ilmn-dragen-1kgp..> Accessed: 2021-7-19.

- Keightley, P D and W G Hill (1988). “Quantitative genetic variability maintained by mutation-stabilizing selection balance in finite populations”. en. In: *Genet. Res.* 52.1, pp. 33–43.
- Kimura, M (1957). “Some problems of stochastic processes in genetics”. In: *Ann. Math. Stat.*
- Kimura, Motoo (1969). “The Number of Heterozygous Nucleotide Sites Maintained in a Finite Population Due to Steady Flux of Mutations”. In: *Genetics* 61.4, pp. 893–903.
- McVicker, Graham, David Gordon, Colleen Davis, and Phil Green (2009). “Widespread genomic signatures of natural selection in hominid evolution”. en. In: *PLoS Genet.* 5.5, e1000471.
- Murphy, David A, Eyal Elyashiv, Guy Amster, and Guy Sella (2022). “Broad-scale variation in human genetic diversity levels is predicted by purifying selection on coding and non-coding elements”. In: *Elife* 11, e76065.
- Nicolaisen, Lauren E and Michael M Desai (2013). “Distortions in Genealogies due to Purifying Selection and Recombination”. en. In: *Genetics* 195.1, pp. 221–230.
- Nordborg, Magnus, Brian Charlesworth, and Deborah Charlesworth (1996). “The effect of recombination on background selection*”. In: *Genet. Res.* 67.02, pp. 159–174.
- O’Fallon, Brendan D, Jon Seger, and Frederick R Adler (2010). “A continuous-state coalescent and the impact of weak selection on the structure of gene genealogies”. en. In: *Mol. Biol. Evol.* 27.5, pp. 1162–1172.
- Price, G R (1970). “Selection and covariance”. In: *Nature*.
- Robertson, Alan (1966). “A mathematical model of the culling process in dairy cattle”. In: *Anim. Sci.* 8.1, pp. 95–108.
- Santiago, E and A Caballero (1995). “Effective size of populations under selection”. en. In: *Genetics* 139.2, pp. 1013–1030.
- (1998). “Effective size and polymorphism of linked neutral loci in populations under directional selection”. en. In: *Genetics* 149.4, pp. 2105–2117.
- Santiago, Enrique and Armando Caballero (2016). “Joint Prediction of the Effective Population Size and the Rate of Fixation of Deleterious Mutations”. en. In: *Genetics* 204.3, pp. 1267–1279.
- Siepel, Adam et al. (2005). “Evolutionarily conserved elements in vertebrate, insect, worm, and yeast genomes”. en. In: *Genome Res.* 15.8, pp. 1034–1050.
- Turelli, Michael and N H Barton (1990). “Dynamics of polygenic characters under selection”. In: *Theor. Popul. Biol.* 38.1, pp. 1–57.
- Wakeley, John (2009). *Coalescent Theory: An Introduction*. Roberts and Company Publishers.
- Walsh, Bruce and Michael Lynch (2018). *Evolution and Selection of Quantitative Traits*. en. Oxford University Press.
- Woolliams, J A, N R Wray, and R Thompson (1993). “Prediction of long-term contributions and inbreeding in populations undergoing mass selection”. In: *Genet. Res.* 62.3, pp. 231–242.
- Wray, N R and R Thompson (1990). “Prediction of rates of inbreeding in selected populations”. en. In: *Genet. Res.* 55.1, pp. 41–54.
- Wright, Sewall (1938). “Size of population and breeding structure in relation to evolution”. In: *Science* 87.2263, pp. 430–431.